



Effects of Different Size of Disc Needle Injury on the Biomechanical Properties of the Lumbar Disc

A Thesis

Presented by

Zijie Wang

Supervisor: Associate Professor John Costi, Michael Russo

Submitted in partial fulfilment of the requirements of the degree of

Master of Engineering (Biomedical)

College of Science and Engineering

Flinders University

May 2020

Declaration

I certify that this thesis does not incorporate without acknowledgement any material previously submitted for a degree or diploma in any University; and that to the best of my knowledge and belief it does not contain any material previously published or written by another person except where due reference is made in the text.

Signed: _____ On: 31 / 05 / 2020

Zijie Wang

Acknowledgements

I would like to express my sincere gratitude to my supervisors, Associate Professor John Costi, and Michael Russo, for their guidance, encouragement and patience throughout my project. I would like to thank them for the support they provided especially under the situation of COVID-19. Lastly and most importantly, I would like to thank all my family and friends for the continued support.

Abstract

Background

Lower back pain is one of the most commonly seen back issues in Australia, disc problems such as disc herniation or disc degeneration can lead to back pain. To find out which one or more damaged discs are causing the pain, discography is needed and served as a surgical diagnostic tool which has been used for the last few decades. Discography includes contrast agent insertion through needle injection as part of the clinical procedure, and it is suggested that acceleration of disc degeneration may occur even with very small needle in modern discography. A two needle system is applied in discography to reduce the chance of discitis, 18G or 20G, 3.5 inch introducers and 22G or 25G, 6 inch inner needle are recommended for discography in different region of spine.

Objectives

The primary aim of this thesis was to assess the effects of different sizes of needle injury on the biomechanical properties of sheep lumbar FSUs. The properties evaluated include the stiffness and energy absorption by 6 Degree of freedom (6DOF) tests before and after 25G and 30G needle injury.

Methods

Healthy sheep lumbar functional spine units (FSUs) in from lumbar region with posterior elements removed (n = 12), L4-5 (n = 3) and L2-3 (n = 9) of similar disc diameter and height were randomly divided into 2 groups: (1) 25G group (n = 6) and (2) 30G group (n = 6). The needle was inserted into the discs through the posterolateral pathway. 6DOF tests were carried out before and after needle injury. The 6DOF biomechanical properties of each group were calculated and analysed using MATLAB in terms of stiffness and energy absorption. Statistical analysis in terms of paired t-test was conducted to investigate if there is significant difference between before and after needle injury.

Results

No significant difference was found in stiffness due to the needle injury apart from the anterior-posterior shear stiffness in 25G group ($p = 0.048$) where the stiffness significantly decreases after induced needle injury. No significant difference was obtained in terms of energy absorption.

Conclusion

These findings suggest that relatively small needle injury does not induce significant changes in the discs in terms of 6DOF biomechanical properties.

Table of Contents

Declaration	I
Acknowledgements	II
Abstract	III
List of Figures.....	VII
List of Tables	X
Chapter 1: Introduction	1
Chapter 2: Literature review	4
2.1 Background.....	4
2.2 Lumbar discography	4
2.3 Current state of disc needle injury studies	6
2.4 Animal model choosing.....	8
Chapter 3: Aims	11
3.1 Proposed project.....	11
3.2 Final project.....	11
Chapter 4: Methodology	12
4.1 Proposed project.....	12
4.1.1 Fatigue and failure.....	13
4.1.2 Needle Injury	14
4.2 Final project.....	15
4.2.1 Specimen preparation	15
4.2.2 Potting	16
4.2.3 6 DOF Testing.....	17
4.2.4 Needle injury	19
4.3 Data and statistical analysis	19
4.3.1 Stiffness	21

4.3.2 Hysteresis zeroed loss area/coefficient.....	22
4.3.3 Phase angle.....	22
4.3.4 Overnight compressive preload	22
Chapter 5. Results	23
5.1 General plots and comparisons	23
5.2 Stiffness	34
5.3 Hysteresis zeroed loss area and coefficient.....	37
5.4 Phase angle.....	40
5.5 Overnight preload comparison	42
Chapter 6. Discussion.....	43
Chapter 7. Conclusion	47
Appendices	48
Appendix A Table of literature review summary	48
Appendix B Code of General plot.....	52
Appendix C Code of comparison plot.....	56
Appendix D Code of overnight preload comparison.....	61
Appendix E Phase angle calculation.....	64
Appendix F t-test result of each DOF	66
Appendix G Displacement over time and force over time plot of overnight compressive preload	69
Reference.....	71

List of Figures

<i>Figure 1. Needle gauge specification</i>	5
<i>Figure 2. Lumbar discography</i>	5
<i>Figure 3. Timeline for mechanical intervention protocol¹⁴</i>	7
<i>Figure 4. Experiment design</i>	13
<i>Figure 5 Lumbar discography through the posterolateral approach</i>	14
<i>Figure 6. The needle position Left: inserting the needle into the disc using posterior lateral approach; Right: confirming the needle is positioned in the centre of the disc.</i>	14
<i>Figure 7 Disc and disx measurement</i>	17
<i>Figure 8(a) and (b) Flinders Medical Hexapod robot machine³⁹, (c) Coordinate system</i>	18
<i>Figure 9. Example of the last cycle of the 6DOF testing curve</i>	20
<i>Figure 10. Example of raw 6DOF testing data of left and right 4° lateral bending test applied to a typical FSU specimen. Displacement (a), rotations (b), forces (c), moments (d), and moment-rotation (e) for a representative specimen that underwent testing at a sinewave frequency of 0.05 Hz. All cycles are shown (e) with the final cycle (red line) used for data analysis.</i>	23
<i>Figure 11. Comparison of last cycle before and after 25G or 30G needle puncture injury of lateral bending tests. (a) Before 25G needle injury, (b) After 25G needle injury, (c) Before 30G needle injury, (d) After 30G needle injury. Legend identifies specimen ID numbers.</i>	24
<i>Figure 12. Example of raw 6DOF testing data of ±3° axial rotation test applied to a typical FSU specimen. Displacements (a), rotations (b), forces (c), moments (d), and moment-rotation (e) for a representative specimen that underwent testing at a sinewave frequency of 0.05 Hz. All cycles are shown (e) with the final cycle (red line) used for data analysis.</i>	25
<i>Figure 13. Comparison of last cycle before and after 25G or 30G needle puncture injury of axial rotation tests. (a) Before 25G needle injury, (b) After 25G needle injury,</i>	

(c) Before 30G needle injury, (d) After 30G needle injury. Legend identifies specimen ID numbers.	26
Figure 14. Example of raw 6DOF testing data of 3° flexion-extension test applied to a typical FSU specimen. Displacement (a), rotations (b), forces (c), moments (d), and moment-rotation (e) for a representative specimen that underwent testing at a sinewave frequency of 0.05 Hz. All cycles are shown (e) with the final cycle (red line) used for data analysis.	27
Figure 15. Example of raw 6DOF testing data of 0.6mm left-right lateral shear test applied to a typical FSU specimen. Displacement (a), rotations (b), forces (c), moments (d), and moment-rotation (e) for a representative specimen that underwent testing at a sinewave frequency of 0.05 Hz. All cycles are shown (e) with the final cycle (red line) used for data analysis.	27
Figure 16. Comparison of last cycle before and after 25G or 30G needle puncture injury of left and right lateral shear tests. (a) Before 25G needle injury, (b) After 25G needle injury, (c) Before 30G needle injury, (d) After 30G needle injury. Legend identifies specimen ID numbers.	29
Figure 17. Example of raw 6DOF testing data of 0.6mm anterior-posterior shear test applied to a typical FSU specimen. Displacement (a), rotations (b), forces (c), moments (d), and moment-rotation (e) for a representative specimen that underwent testing at a sinewave frequency of 0.05 Hz. All cycles are shown (e) with the final cycle (red line) used for data analysis.	30
Figure 18. Comparison of last cycle before and after 25G or 30G needle puncture injury of left and right lateral shear tests. (a) Before 25G needle injury, (b) After 25G needle injury, (c) Before 30G needle injury, (d) After 30G needle injury. Legend identifies specimen ID numbers.	31
Figure 19. Example of raw 6DOF testing data of compression tests applied to a typical FSU specimen. Displacement (a), rotations (b), forces (c), moments (d), and moment-rotation (e) for a representative specimen that underwent testing at a sinewave frequency of 0.05 Hz. All cycles are shown (e) with the final cycle (red line) used for data analysis.	32
Figure 20. Comparison of last cycle before and after 25G or 30G needle puncture injury of compression tests. (a) Before 25G needle injury, (b) After 25G needle injury,	

(c) Before 30G needle injury, (d) After 30G needle injury. Legend identifies specimen ID numbers.33

Figure 21. Bar chart showing the averaged stiffness of each DOF except for flexion-extension, taken from Table 1. (a) Right Lateral shear; (b) Left lateral shear; (c) Anterior shear; (d) Posterior shear; (e) Compression; (f) Right Axial Rotation; (g) Left Axial Rotation; (h) Right Lateral Bending; (i) Left Lateral Bending.36

Figure 22 Bar chart showing the Averaged hysteresis loss area of each DOF with SD except for flexion-extension. (a) Left and Right Lateral shear; (b) Anterior-posterior shear; (c) Compression; (d) Axial rotation; (e) Lateral bending.39

Figure 23 Bar chart showing the Averaged phase angle of each DOF with SD except for flexion-extension. (a) Left and Right Lateral shear; (b) Anterior-posterior shear; (c) Compression; (d) Axial rotation; (e) Lateral bending.41

Figure 24 Displacement over time of 25G needle injury group overnight compressive preload. Specimen data before and after needle injury is plotted in the same color, the thick solid line represents the intact data, the dotted thin line represents the injured data.42

List of Tables

<i>Table 1. Averaged ‘positive region’ and ‘negative region’ stiffness of each DOF with standard deviation. The unit of lateral shear, anterior-posterior shear, and compression is N/mm; The unit of axial rotation, lateral bending, and flexion-extension is Nm/°.....</i>	<i>34</i>
<i>Table 2 Averaged Hysteresis loss area of each group before and after needle injury of each DOF. The unit is Jules.....</i>	<i>37</i>
<i>Table 3 Averaged Hysteresis loss coefficient of each group before and after needle injury of each DOF. No unit.....</i>	<i>37</i>
<i>Table 4 Averaged Phase Angle of each group before and after needle injury of each DOF. The unit is °.....</i>	<i>40</i>

Chapter 1: Introduction

Lumbar discography is a commonly used procedure when other non-invasive diagnostic methods have not successfully diagnosed the source of low back pain (LBP). Needle puncture of the disc for contrast agent insertion is part of the clinical procedure of discography. A two-needle system with a 22-gauge 7-inch spinal needle is inserted via the 18-gauge 3.5-inch spinal needle to protect the very small needle from bent or break while puncturing through the musculature when a lumbar discography is performed¹.

Many articles have studied the extent of needle puncture injuries with different needle diameters^{2,3,4}, injection volume or types of contrast agents⁵ induce changes in the discs (see [section 2.3](#)). Human intervertebral discs can be difficult to acquire due to the ethical and government regulatory restriction, and of the challenges with obtaining 'young and healthy' cadaver discs. Hence, animal models like sheep, mouse, bovine and rabbit of lumbar region or tail⁶ are applied as a substitute which has relative similar anatomy of spine⁷, loading and size, mechanical⁸, biochemical⁹ properties comparing to the human spine after scaling. Elliot et al. concluded that the mechanical properties may be changed after needle puncture according to the nucleus pulposus depressurization and/or annulus fibrosus damage which depending on the needle size¹⁰. They found that a ratio of 40% between the needle diameter and disc height can be considered as the threshold of whether there are significant changes from 23 in vivo studies using rat, rabbit, dog, or sheep studies¹⁰.

The functional spine unit (FSU) or motion segment is one of the most commonly used terms in disc studies. The FSU is the smallest physiological motion unit of spine to exhibit biomechanical characteristics similar to those of the entire spine¹¹. The FSU is comprised of the disc and adjacent vertebral bodies, posterior elements and ligaments. In vitro studies of isolated or multiple FSU's are often used to measure biomechanical properties of the spine.

A ten-year well-matched cohort study from Carragee et al. in 2009 found that discs that had been exposed to puncture and injection during discography had greater progression of degenerative findings compared to control discs¹². More than double

the rate disc herniation occurred in the discography group compared to control group. Significantly greater loss of disc height ($p = 0.05$) and signal intensity ($p = 0.001$) were found in the discography group compared to the control disc¹². This study suggested that accelerated disc degeneration, disc herniation and loss of disc height can occur even using modern discography techniques with small gauge needle and limited pressurization.

Also, many other articles in the past two decades have investigated how different sizes of needle affect the disc's biomechanical properties and whether the needle puncture would induce degeneration of the disc by evaluating radiographic, MRI related, biological, histological, chemical properties^{13, 14, 15} (see [section 2.3](#)). No articles have focused on how human labour activities affect the disc mechanical properties after needle puncture as it is hard to simulate those activities in a testing environment with acceptable accuracy with hybrid position-load control.

To investigate how human labour activities affect the disc properties before and after needle injury, the proposed project aims are to investigate the effect of intervertebral disc needle injury and fatigue on 6 degrees of freedom (DOF) biomechanics and failure properties using sheep's lumbar spine in the Flinders Medical Hexapod Robot. Unfortunately, the COVID-19 broke out just a week before the laboratory practical testing starts. The University did not shut down the laboratory or master's research projects, however, to obey the social distancing requirements as a master student (by coursework), the author and supervisors decided to change the proposed project into data analysis of previous related experimental tests as the final project. A comprehensive literature review and experiment design were achieved for the proposed project. Most of the finding from the literature review were applicable to the final project. The final project, in short, is a data analysis of 6 DOF biomechanical properties on previous needle injury tests of sheep lumbar FSUs with more depth.

This thesis was divided into 6 main sections:

- Literature review: Comprehensive review of the current literature on human lumbar discography, research techniques for needle injuries, animal model

selection, scaling of injury size for animal models and intervertebral disc properties.

- Aims: The aims of proposed project and final project are presented.
- Methodology: Experimental design and how it is related to the research aims. Flinders Hexapod Robot 6DOF and failure testing procedure, data analysis. Description of developed aims for the proposed project and complete methods of the final project.
- Results: a presentation and explanation of the results, detailing stiffness, energy absorption and overnight compressive pre-load.
- Discussion: Discussion of the results, how the results relate to the research aims and previous studies, limitations of the research.
- Conclusions: highlight the main findings and their relation to the aims of the study. Discussion of future works.

Chapter 2: Literature review

This section indicates the summary of all articles that are relevant to the adverse effect of disc needle injury and the considerations on this project's design according to the literature review. Three parts will be presented: Background including the lumbar discography, the current state of disc needle injury studies and animal models choosing for the experiment. A brief introduction of experiment design that indicates choosing the needle diameter, animal model selection, and assessment of the 6 DOF biomechanics and failure properties.

2.1 Background

According to the latest data from the Australian Institute of Health and Welfare (AIHW) in 2019, different levels of back problems occur in every 1 in 6 Australians¹⁶. Among all the back issues, discs problems (herniated discs or disc degeneration) are always included. To find the most appropriate treatment for the back issues, it is critical to detect which one or more discs are causing the discomfort. Discography is a surgical diagnostic technique that could identify the "damaged" intervertebral disc in the patient that is causing lower back pain¹⁷. This commonly used method includes contrast media injection into the nucleus which is the needle injection procedure, and the adverse effect of this procedure on discs has been discussed and studied over the last two decades by researchers^{10,18}. Other radiographic techniques can also be employed to diagnose disc degeneration but cannot provide information on which particular disc or discs are responsible for the patients' lower back pain.

This thesis project is focusing on how needle injury (caused by needle injection procedure) and the fatigue afterwards affect the biomechanical and failure properties of lumbar disc. Human discs are rare and expensive, the animal model will be used instead in this project. The Flinders Hexapod Robot will be employed to carry out the fatigue simulation, biomechanical assessment, and failure test. MATLAB will be used as the major analysing tool for 6DOF biomechanics and failure data.

2.2 Lumbar discography

Lumbar discography is also called disc stimulation or provocation discography. It acts as the diagnostic method for detecting the discomforted disc that is causing lower

back pain. With the post discography CT, the disc which is causing the clinical pain can be identified and anatomical lesion of the disc can be located and evaluated. This is a powerful and commonly used method to diagnose lower back pain and multiple disc levels can be evaluated using this technique¹⁹.

For the technique in the lumbar region, lumbar discography has developed from a pure posterior approach in the 1940s to the lateral and posterolateral approaches that are commonly used nowadays²⁰. For patient positioning, the posterolateral approach includes placing the patient's body slightly oblique, rotated forward, and at a 45-degree angle to the bed²¹. This project will use cadaveric animal models thus more attention is on the needle placement. A two-needle system with the posterolateral approach is used for clinical human lumbar discography²². A 3.5-inch long large needle (18-gauge to 20-gauge) is inserted through the musculature, and a 7-inch small needle (22-gauge to 24-gauge) will be inserted through the large needle (Figure 1.).

This image has been removed due to copyright restriction. Available online from

[\[https://images.app.goo.gl/8NUFGbSHicjzE7eXA\]](https://images.app.goo.gl/8NUFGbSHicjzE7eXA)

Figure 1. Needle gauge specification

The two-needle system is applied to protect the fragile small needle from breakage. The needle tip should be in the centre of the disc space. This procedure can be duplicated for all the levels to be tested if needed.

This image has been removed due to copyright restriction. Available online from

[\[https://images.app.goo.gl/GQGypSNRKTyLgg3M8\]](https://images.app.goo.gl/GQGypSNRKTyLgg3M8)

Figure 2. Lumbar discography

An annular hole is generated after needle puncture and it remains unclosed (Figure 2), this will cause several adverse responses around the injury site. The disc properties will be influenced in theory if that hole exists and the level of the effect depends on a lot of factors, such as the needle diameter, disc degeneration status, and so on²³. This thesis project only focusses on the effect of needle size on the

intervertebral disc, and the summary of former studies is presented in the next section.

2.3 Current state of disc needle injury studies

Discography may accelerate the process of disc degeneration because of the structural destruction due to its needle injection procedure, delamination according to the fluid injection or cell death due to the adverse response of the infected agent². Those hypotheses of acceleration on disc degeneration due to discography were not investigated quantitatively on human subjects until a ten-year matched prospective cohort study that focuses on the disc degeneration progression with and without baseline discography is published in 2009²⁴. This study has many good features that make it a very good reference, for instance, human subjects, long-term performance investigation, prospective in its nature. This study suggested that modern discography techniques were likely to cause acceleration in disc degeneration, disc herniation, loss of disc height and signal even with small gauge needle and limited pressurization. Another in-vitro study suggested that the risk of acute herniation through the puncture site is dependent on the needle diameter used²⁵ which support the hypothesis of this thesis. 25-Gauge and 18-gauge needle were used to create structural damaged by obtaining progressive, the full transverse cross-section of healthy ovine lumbar discs entire height. They concluded that the lateral inner annulus was the most vulnerable site to disruption. Another important study by Elliott et al. proposed that significant disc properties changes may not be obtained if the needle diameter: disc height ratio is less than 40% after summarized 17 other studies with their own experiments using rat²⁶, rabbit^{2,27}, and sheep¹⁰. This ratio of needle diameter and disc height guides the needle selection of this thesis's experiment design.

Many other studies have also investigated the acceleration on disc degeneration due to needle injection in the last two decades^{24- 30}. The studies that focused on how needle injury changes the discs' properties were found to be useful. Among all the articles, three factors are mostly being considered for altering the effect of needle injection:

- Needle diameter;
- Volume of contrast agent;
- Type of contrast agent.

In this thesis, the author will only focus on the needle diameter thus sham injection technique is applied to get rid of the effect of the contrast agent. Sham injection means that no actual contrast agent is inserted into the disc through the needle after the puncture. In this case, the literature search focused on the “disc needle injury” and “needle size effect”. A table of summary indicates the critical information of relevant previous articles is presented in [Appendix A](#).

For most of the studies, animals will be harvested if the discs structural and functional properties were investigated because it is almost impossible to carry out these tests if the subject is alive. One particular study that investigated the effect of needle puncture injury on intervertebral disc mechanics and biology in an organ culture model which can be considered to be “in vivo”¹³. 25G and 14G needles were used with a posterolateral approach into the bovine intervertebral disc in organ culture. Compression loading protocol for simulation of daily human activity was applied after the puncture, the structural and functional properties were assessed before and after needle puncture (Figure 3.). They concluded that immediate and progressive changes caused by improper implications of discography can be detected in the disc in both mechanical and biological perspectives.

This image has been removed due to copyright restriction. Available online from

<https://www.ncbi.nlm.nih.gov/pmc/articles/PMC2587060/>

Figure 3. Timeline for mechanical intervention protocol¹⁴

Another in vitro biomechanical study using rabbit lumbar FSUs suggested that disc puncture and stab might reduce the neutral zone stiffness and increase the range of motion in flexion/extension³¹. The stiffness changes can be examined in this thesis. 16G needle using the anterolateral approach and 11G blade was inserted laterally on the left side to the full disc width; destructive testing load-to-failure and non-destructive testing flexibility testing were carried out in this article. A mouse model

was used in a study in 2013. Two much smaller needle 29G (65%-disc height) and 26G (90%-disc height) were used in this study due to the small animal model. Compression/tension data were analysed for compressive stiffness and range of motion (ROM), their testing protocol consisted of 20 cycles of compression/tension from -1.5 to +0.5N at 0.5Hz and 10 cycles of torsion of $\pm 8^\circ$ at 0.05Hz.

From literature searching, it is found that studies tend to investigate the compressive stiffness, tension stiffness by analysing the loading-unloading cycle if focusing on the biomechanical perspective. However, the author found a very limited number of articles that investigated how fatigue and needle injury affects all 6DOF. Besides, it is found that researchers tend to use needles with a huge diameter difference for a more significant difference in comparison. Sometimes even 90% of the disc height, which is more like the stab model instead of needle puncture model. Unlike needle injury puncture model, the stab model is mostly used to create severe damage. For instance, Hartman et al. (2015) used a No. 11 scalpel blade to serve as a positive control for severe damaged, the blade was inserted laterally on the left side to the full disc width. Their stab model is similar to the injury model used by Lipson and Muir³².

2.4 Animal model choosing

Human material for this study is difficult to get because of both ethical and political regulatory restriction, in this case, cadaveric animal models and in vivo models were commonly used. Most publications used small animal models, for instance, rat, mice, and rabbits ([Appendix A](#)). The reason is that compared to large animal models, small animal models are not as expensive and can be easier to get. Hence, the majority of studies chose small animals for spine/disc research.

One consideration of this experimental design is the needle selection, small animal model like mouse's disc is very sensitive to needle puncture even with a small needle diameter (less than 10% of the disc height)⁹. This makes the choice of animal model a critical factor as there are advantages and disadvantages to compromise.

To select appropriate animal model, criteria like the development and anatomy of the spine, loading and size differences, mechanical, biochemical, nutritional

properties need to be considered⁶. Alini et al. suggested that most of the animal models can be useful in some specific aspect of disc biology with a clear scientific question. For instance, this project focus on the biomechanical properties, then an animal model with relative similar response through mechanical interventions can be chosen.

A study in 2008 compared the normalized axial mechanical properties between 9 disc types in 7 mammalian species and human⁸. The 9 disc types include calf, pig, baboon, sheep, rabbit, rat and mouse lumbar, and the cow and rat tail. They concluded that disc axial mechanics are very similar across animal species after normalizing by the disc height and area. They found that the goat and mouse discs are the most similar ones from a normalized torsional perspective, while pig and sheep discs were the least similar ones. Another research by O'Connell et al. compared the normalized disc geometry parameters (disc height, lateral width, AP width, area etc.) and ranked them³³. The animal model that most similar to human are the rat tail (46%) followed by sheep (31%). There is another study that first studied the similarity between sheep spine and human spine from the biomechanical aspect and pointed out that sheep spines may be a valid biomechanical model for human spines³⁴. A single functional spine unit (FSU) was tested under pure moments in the three main anatomic planes, and the results showed that the craniocaudally variation in the range of motion in all load directions were similar between sheep spines and values reported in the literature for human specimens. When considering biomechanical properties, water content, collagen content of the annulus and collagen fibre orientation angles should be considered as they are responsible for both axial and rotational stiffness. According to Reid et al., sheep lumbar intervertebral discs are a reasonable choice as models for human discs when focusing on the biomechanical properties³⁵.

The possibility of using kangaroo as the alternative for disc research has been discussed recently, morphological characteristics similarity between kangaroo lumbar intervertebral disc and human intervertebral disc were compared and they suggested that kangaroo can be an appropriate selection³⁶. Kangaroo may be hard to find or harvest in other countries, but in Australia, kangaroo is possible.

Several potential animal selections were identified according to the literature review, sheep (lumbar region), rat (tail), or bovine (caudal region). These animal models are all proper for spine/disc research as they are the most similar ones comparing to human spine in both anatomical and mechanical aspects.

Any differences in dimensions can be easily allowed for in the design of a mechanical test, for instance, adjusting the load subjected on sheep discs to the same stress subjected on human disc in a compression test under load control. The purpose of the proposed and final project is all focused on the analysis of disc biomechanical properties. Hence, animal models that have the most similar biomechanical properties should be chosen. FSUs from sheep lumbar spine (L4-5) was finally selected for proposed project as it has similar mechanical and geographical properties comparing to human lumbar disc according to the literature review. The sheep lumbar disc was also used for final project.

Chapter 3: Aims

The aims of the proposed project are presented (Section 3.1). Unfortunately, due to COVID19 these aims had to be adjusted to fit the data form the Final project (Section3.2).

3.1 Proposed project

According to the literature review, the aims of the proposed project are:

Aim 1: Determine if one day of labour activities affect the 6DOF mechanics of the intervertebral disc

Aim 2: Investigate the effect of needle injury on 6DOF intervertebral disc biomechanical properties.

Aim 3: Investigate the effect of needle injury on 6DOF intervertebral disc biomechanical properties after fatigue.

Aim 4: Investigate how failure properties change after needle injury and fatigue.

3.2 Final project

The aims of the final project are:

Aim 1: Investigate how different sizes of needle affect the disc 6 DOF biomechanical properties.

Aim 2: Developing MATLAB code for investigation of 6DOF biomechanical properties.

Aim 3: Determine if the overnight compressive preload was sufficient for reaching steady-state

Chapter 4: Methodology

The proposed methods were developed prior to project scope change. These methods are described (section 4.1) for the future continuation of the project, once it is safe to do so. The experimental data of the final project (section 4.2) was from another researcher in the group as part of a similar study. Methods from the final project design were similar to the proposed methods, specimen preparation, testing fixation, needle injury approach, and 6DOF testing were consistent between the two studies. Research and methodology development for fatigue and failure testing of FSU's was continued. These methods are described but were not used in the final project initial methodologies.

Data analysis methods were developed specifically for the final project data (section 4.3). The methods used would be similar if future projects were to implement them for the proposed study design.

4.1 Proposed project

This section will introduce the experiment design of the proposed project in brief according to the aims. Needle diameter selection, injection approach, animal model selection, 6 DOF (right/left lateral shear, anterior/posterior shear, compression, extension/flexion, right/left lateral bending and axial rotation; Section 4.3.3) biomechanical properties and failure properties assessment, and fatigue simulation design are discussed.

Needle diameter with 40% of the disc height and 7% of the disc height was chosen. 40% of the disc height is the threshold of whether there is a significant change in the disc, 7% of the disc height indicates the needle diameter and human disc ratio that used in clinical lumbar discography. A posterolateral injection approach is applied to follow the state-of-art of the clinical lumbar discography. The needle was pushed through the disc annulus with a constant force; sham injection technique is applied; no agent is injected into the disc to get rid of the effect of the pressurized fluid agent.

Sheep lumbar spine was selected as the specimen for the experiment. Small animal models were cheap and easy to find but hard to manipulate by the Hexapod machine because of the small sample size.

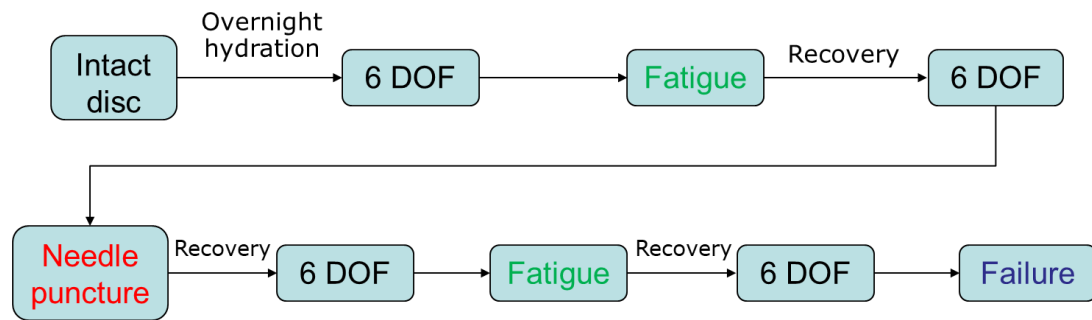


Figure 4. Experiment design

The whole experiment design can be separated into two stages: before needle puncture and after needle puncture (Figure 4.).

Part 1: Before the needle injury, the 6DOF test results before and after fatigue;

Part 2: After the needle injury, the 6DOF test results before and after fatigue.

4.1.1 Fatigue and failure

The fatigue will be simulating one-day human labour activity, and the recovery process will be simulating one-night rest. All the 6 DOF biomechanical and failure testing will be carried out on the Flinders Hexapod machine. Compressive stiffness, ultimate force, and energy absorption will be calculated. The failure test will be carried out at last. Same disc will be used from the beginning to the end. The same disc will be used to finish throughout the whole experiment, hence, whether fatigue affects the healthy disc's properties can be investigated before needle injury. A healthy disc should be fully recovered after fatigue, in this way, how fatigue affects the disc after needle injury can be discussed. The whole experiment for one specimen will take about 15 hours.

1-day human labour activities are simulated as the fatigue, and 1-night sleep is simulated as the recovery. 7 hours actual working hour is reasonable in Australia, for labour work, 1 task per minute gives $7\text{h} \times 60\text{min} = 420$ cycles for each fatigue process. 13° flexion with 2° axial rotation at 1 Hz with hybrid position/load control in the other DOFs applied to prevent the unwanted moments. 1.1MPa of compressive disc pressure applied to simulate holding a 20Kg box with normal

posture. A 6DOF mechanical properties testing is carried out after the fatigue and 30-minutes recovery.

After the final 6DOF test, specimens were moved to their loading group posture and failed axially at 400 mm/min³⁷.

4.1.2 Needle Injury

Two sizes of needles are selected for the needle injury, which are 7% and 40% of the disc height. As mentioned in the literature review, 7% of the disc height is the needle gauge used for human lumbar discography, 40% of the disc height is the needle gauge that found to be the threshold for whether there is a significant change in the disc properties after needle injury¹⁰. No contrast agent is injected into the disc. The former data applied 25G and 30G needle through a posterolateral approach (Figure 5).

This image has been removed due to copyright restriction. Available online from

<https://images.app.goo.gl/E7UEPykNcZL3CoZSA/>

Figure 5 Lumbar discography through the posterolateral approach³⁸

A posterolateral approach is used for needle injection, and most institutions, nowadays, carrying out discography with high-resolution C-arm as the imaging guide for needle placement³⁹. To simplify the procedure, no C-arm is applied for the needle injury. The needle position as it approaches the disc using a posterior lateral approach (Figure 6.left). Once anterior to the superior articular process, the needle is steered medially to enter the disc⁴⁰. Once the annulus is punctured, then confirming the needle is positioned in the centre of the intervertebral disc (Figure 6. right).

This image has been removed due to copyright restriction. Available online from

<https://www.birpublications.org/doi/pdf/10.1259/0007-1285-51-607-498>

Figure 6. The needle position Left: inserting the needle into the disc using posterior lateral approach; Right: confirming the needle is positioned in the centre of the disc⁴¹.

To maintain the needle injection constant and make sure that the needle is through the annulus fibrosus, the needle was injected approximately in the centre of the disc for each specimen.

4.2 Final project

Unfortunately, to follow the social distancing and other safety requirements from SA government and Flinders University due to the COVID-19, the proposed study was not feasible. Hence, the proposed project's aims and directions were changed to focus on the data analysis instead of laboratory-based practical experiments. Hence, data analysis on former experimental data of 12 sheep specimens before and after 25G or 30G needle injury was performed with more depth. All the data analysing methods and skills are applicable to the original experiment as stiffness, energy absorption are the two aspects that being focused on when analysing the last cycle of each DOF. The whole 12 specimens have an average disc height of 5.10mm.

Group 1: Before and after 25G (10.2% disc height) needle injury (n = 6);

Group 2: Before and after 30G (6.2% disc height) needle injury (n = 6).

In this section, the specimen preparation, potting, 6DOF testing, fatigue, needle injury, failure, and data analysis will be introduced.

4.2.1 Specimen preparation

Due to the shortage of storage of sheep lumbar spine, it was hard to find enough L4-5 specimens with similar size. Hence, 12 sheep lumbar segments with similar dimensions were found by measuring the X-Ray image and dissected afterwards, the surrounding soft tissue was removed. The facet joint capsules, anterior ligament, posterior longitudinal ligament, and posterior elements were kept intact to keep the project clinically relevant. All the Lumbar spine were sorted at -30°C (-22°F) and then defrosted at room temperature for at least 3h before the dissection process. The superior and inferior vertebral surfaces were then cut parallel to the mid-transverse plane of the disc and the length from disc to both ends should be roughly 30 mm, using an alignment device in a bandsaw. Then, refrozen the specimens until the day before testing. Again, the specimens need to be taken out of the fridge 3h prior testing.

The former experiments used the same specimen preparation method, and the only difference is that the posterior elements are removed to only focus on the discs' properties.

4.2.2 Potting

Potting is needed before any mechanical testing to make the specimen be able to fit in the Hexapod machine. Firstly, the specimen needs to be dried. Assuring there is no moisture on bone and making sure all soft tissue is off the bone by using a scalpel. Then making sure there is at least 10 mm of exposed bone on superior and inferior bones (including on posterior elements). Also taking Anteroposterior, lateral, and oblique pictures of the specimens with label on them. Two cups were needed, a top cup and a bottom cup, also making sure specimen, cups and alignment rig were in the fume hood for potting in PMMA. Placing specimen into the bottom cup and making sure it is not rotated. Checking the specimen orientation for proper placement of FUS in the potting medium.

For PMMA potting, PMMA powder, Monomer agent, measuring cups, mixing cups, and mixing utensil were needed. Mixing PMMA at a ratio of 2.5 ml Powder to 1 ml liquid. Pouring PMMA into the bottom cup and making sure PMMA is not higher than the bottom lip. After 15 to 20 minutes, the PMMA was hardened.

When bottom-up is potted, measuring the disc measurement (see Figure 7) by using the inner diameter end of the caliper and the disc (see Figure 7) measurement by using the depth end of the caliper. With both disc and disc, the geometric centre can be calculated and recorded.

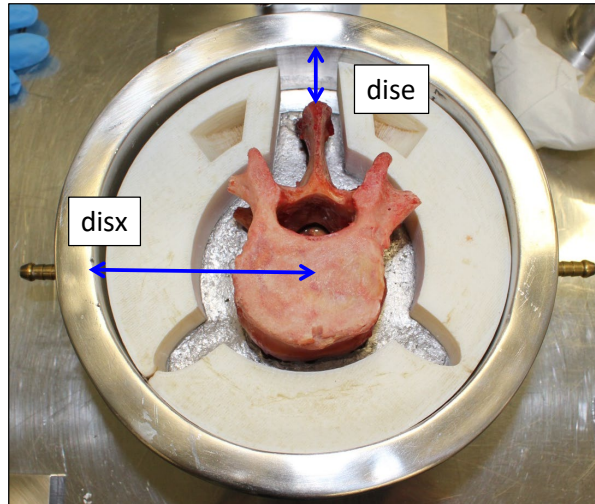


Figure 7 Dise and disx measurement

Attach top cup with alignment plate to rig base and attach bottom cup to slide mount. Similar potting process was done for the top cup, making sure PMMA is 3 mm below tape edge and the right potting height. Allow specimen to cool for 15 minutes⁴².

4.2.3 6 DOF Testing

A custom-developed 6DOF Flinders medical hexapod robot machine was employed to manipulate the embedded FSU with respect to the hexapod's axes (+x =right lateral, +y = anterior, +z = superior). In short, the hexapod robot employs six servo-controlled ball screw driven actuators that can precisely position a mobile upper plate with respect to the fixed base plate. All the mechanical testing will be carried out on the Hexapod robot in this project⁴³ (Figure 8).

The images (a) and (b) have been removed due to copyright restriction. Available online from

<https://images.app.goo.gl/c4kjiD3wNGmcTq7n9>

<https://images.app.goo.gl/VunEmrgedZcprxTd6>

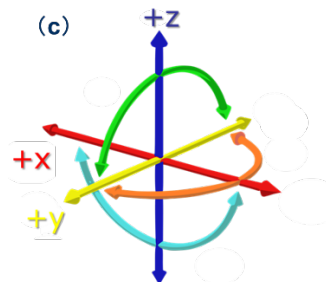


Figure 8(a) and (b) Flinders Medical Hexapod robot machine, (c) Coordinate system

Before testing, proper hydration and temperature are needed as the disc has its viscoelastic tissue properties and they are temperature and hydration dependent^{44,45}. To simulate a similar in vivo environment, the specimens need to be immersed in a 0.15 M phosphate-buffered saline (PBS) bath at 37 °C throughout testing⁴⁶. A 12h axial compression preload that simulating the unloaded lumbar disc during sleeping was performed on the disc with a nucleus pressure of 0.1MPa⁴⁷ in the temperature-controlled bath for hydration equilibrium. A factor of 1.5 is applied for the applied external FSU compressive stress and nucleus pressure (Nucleus pressure = 1.5 External FSU compressive stress). The unloaded disc area was estimated on the formula $0.84 \times AP \times LAT$ ⁴⁸. The AP and LAT represent the largest anteroposterior and lateral dimensions from the inferior and superior vertebrae, averaged over three measurements through the X-Ray image taken before potting.

Then an initial reference compression test was conducted to simulate the in-vivo intradiscal pressure recorded during standing. The 6DOF test then could be carried out afterwards. For the 6DOF test, with the capability of Flinders Hexapod machine, the FSU underwent dynamic haversine displacement/rotation in each DOF with a hybrid position-load control protocol that drove the primary axis in position control while minimizing coupling forces/moments in the other 5DOF via real-time control⁴⁹. Also, the same 0.5MPa follower preload was applied during all 6DOF tests. For the displacement and rotation amplitudes:

- $\pm 0.6\text{mm}$ in all shear tests (anterior and posterior, left and right lateral shear)

- Compression test
- $\pm 4^\circ$ for axial rotations
- $\pm 3^\circ$ for lateral bending
- 3° for flexion and extension.

For each of the test listing below, five cycles at 0.1 Hz were applied, followed by a 2 minutes recover. Rotation vs. Moment and Displacement vs. Force curve in each degree of freedom is generated and investigated from the 6 DOF testing data. All full sin-wave, which means the rotation or displacement goes both positive and negative direction.

4.2.4 Needle injury

25G and 30G needle were used with similar posterolateral approach (section 4.1.2) to create the needle injury on the specimens.

4.3 Data and statistical analysis

The final project focuses on the data analysis of former experimental data, which includes the investigation of stiffness and energy absorption of the intact and injured discs. To be specific, energy absorption was investigated in terms of hysteresis loss area/coefficient, and phase angle. Due to the COVID-19, the data that the final project analysed was from previous related experimental data.

The data investigations were mainly based on the 'last cycle' curve of each DOF (Figure 9.). Investigating the very last cycle from the 6 DOF test is due to the specimens' responses are most likely to reach a steady-state, as earlier cycles give varied responses due to viscoelasticity.

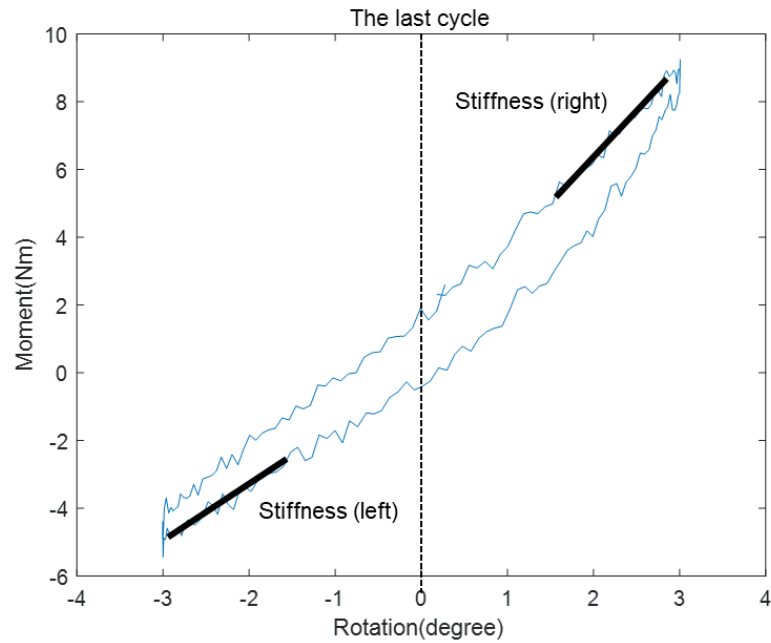


Figure 9. Example of the last cycle of the 6DOF testing curve

Former experimental data includes 12 specimens in total which was separated into 2 groups, one injured with 25G needle and the other with 30G needle. 6 DOF tests were performed for all specimens before and after needle injury, failure tests data were available for a few specimens. The general plot of raw 6DOF data, comparison plot of the smoothed curve between before and after needle injury are both generated. Different from the other tests, the last cycle of compression test was chosen using a 'peak to peak' fashion while others were using 'mid to mid' fashion, due to the very noisy starting and finishing stages of compression tests. The data were smoothed and zeroed for better visual comparison as the raw data has too much noise.

To distinguish whether the data is normally distributed, measures of Skewness and Kurtosis were both carried out on the raw data. Skewness measures the symmetry and Kurtosis measures the 'flatness' of tails. The hypothesis is that the data is normally distributed with a Skewness value of -1 to 1, and a Kurtosis value of -2 to 2. If the data is normally distributed, an independent sample t-test on the calculated results was applied to quantitatively compare whether there is a significant difference between the biomechanical properties before and after needle injury. If

not, the Wilcoxon signed-rank test which is a non-parametric statistical hypothesis test will be applied to investigate whether the mean ranks differ.

Besides, the overnight compressive preloading before and after needle injury were visually compared.

4.3.1 Stiffness

Stiffness is obtained within a particular range of the loading curve (Figure 9.) using linear regression (Polyfit.m, MATLAB® with an order of 1). The target region for slope calculation depends on the magnitude of displacement (mm) and rotation (degree):

- ± 0.6 mm in all shear tests (anterior and posterior shear, left and right lateral shear), stiffness obtained from 0.3mm-0.59mm (both direction)
- Compression test
- $\pm 3^\circ$ for axial rotation, stiffness obtained from 1.5° to 2.9° (both direction)
- $\pm 4^\circ$ for lateral bending, stiffness obtained from 2° to 3.9° (both direction)
- 3° for flexion/extension, stiffness obtained from 1.5° to 2.9°

An averaged stiffness with its standard deviation in each group was calculated for each DOF. 'Positive region' stiffness (Figure 9. 'stiffness right') and 'negative region' stiffness (Figure 9. Stiffness left) were both calculated for Left-right lateral shear, anterior-posterior shear, axial rotation, and lateral bending tests. Compressive stiffness was the only stiffness being considered in the compression test.

To compare whether there is a significant change between before and after needle injury, a one tail, type 3 T-test is performed for normally distributed data. The hypothesis is that the right stiffness after needle injury is significantly different from before needle injury. If $p > 0.05$, reject. If $p \leq 0.05$, accept.

For data that was not normally distributed, the hypothesis is that if the test statistic value is less than the corresponded critical value (Critical value = 2, according to critical values of Wilcoxon Singed Rank test table), then it suggests there is difference between before and after needle injury.

4.3.2 Hysteresis zeroed loss area/coefficient

Hysteresis zeroed loss area is the area under the curve after adjusted the curve to the original point according to rotation or displacement (Figure 9.). The Hysteresis zeroed loss coefficient is the ratio between the area under the curve and the area enclosed by the top half of the curve and the x-axis.

Similar to stiffness, the same type of t-test was carried out to check if there is a significant difference between before and after hysteresis zero loss area/coefficient.

4.3.3 Phase angle

Phase angle gives insight into the viscoelasticity of the intervertebral disc. Phase angle is a measure of the energy absorption behaviour of the spine segment. The higher the value of phase angle is, the more viscoelastic the material is³⁶. A standard code with phase angle calculation function was given by the supervisor.

Similar to stiffness, the same type of t-test was carried out to check if there is a significant difference between before and after phase angle.

4.3.4 Overnight compressive preload

Overnight preloading is equivalent to a nucleus pressure of 0.1MPa which simulate the disc's overnight resting during sleep. Although there is a variance of loading time between before and after needle injury, the plot of displacement or force over time is still comparable to determine whether the needle injury has an effect on the disc resting stage.

All those investigations were performed on MATLAB, and the code of them was mostly generated and analysed by the author and with the help of supervisors. The MATLAB codes that achieve those functions are attached in [Appendix B](#) to [Appendix E](#).

Chapter 5. Results

In this section, the data analysis of results is presented and explained according to each DOF, before and after needle injury (25G or 30G). Following the comparison of the compressive overnight preloading over time, before and after needle injury.

5.1 General plots and comparisons

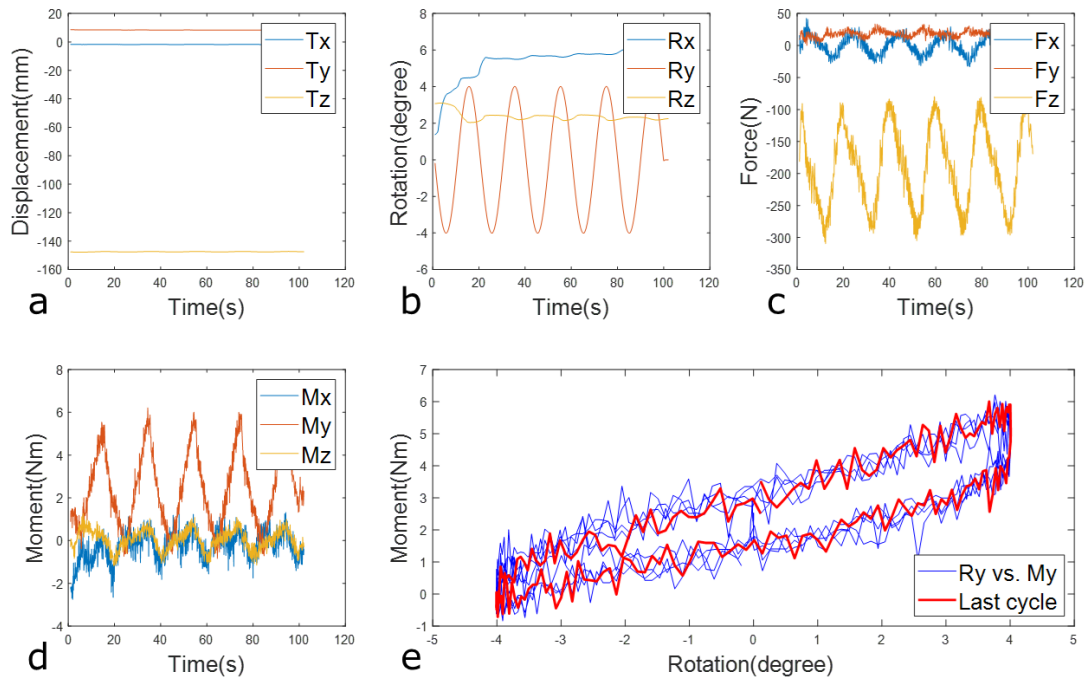


Figure 10. Example of raw 6DOF testing data of left and right 4° lateral bending test applied to a typical FSU specimen. Displacement (a), rotations (b), forces (c), moments (d), and moment-rotation (e) for a representative specimen that underwent testing at a sinewave frequency of 0.05 Hz. All cycles are shown (e) with the final cycle (red line) used for data analysis.

An example of raw 6DOF testing data plot of one typical specimen which indicates how displacements, rotations, forces, and moments changes over time, with a rotation vs. moment curve being plotted to investigate the 0.05 Hz $\pm 4^\circ$ lateral bending test (Figure 10). No displacement is detected in all three directions as this is a rotational test (Figure 10. a). However, some periodic rotation, force, and moment are detected on both x- and z-direction, which is because that the Flinders Medical Hexapod machine has the function of position-load control to minimize the displacement or rotation on every other direction rather than the testing one (Figure

10. b-d). Last cycle of the lateral bending test is highlighted in red (Figure 10. e), stiffness and hysteresis zeroed loss area are all calculated from the last cycle ([Section 4.4](#)).

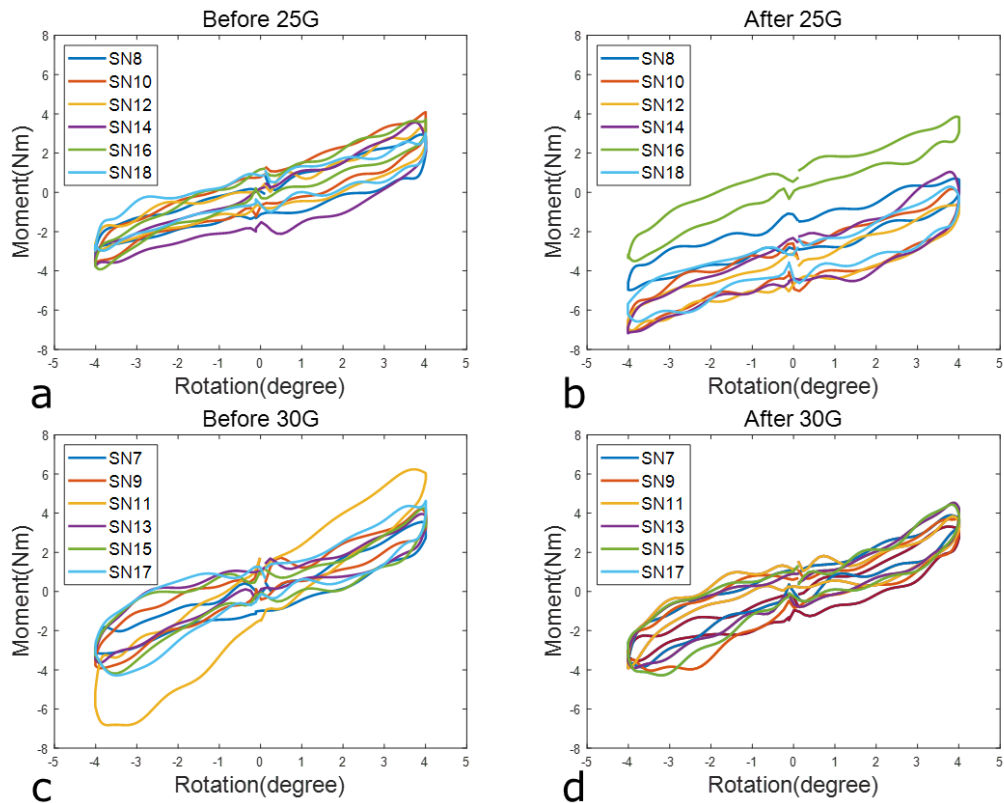


Figure 11. Comparison of last cycle before and after 25G or 30G needle puncture injury of lateral bending tests. (a) Before 25G needle injury, (b) After 25G needle injury, (c) Before 30G needle injury, (d) After 30G needle injury. Legend identifies specimen ID numbers.

The loading-unloading curves after 25G needle injury (Figure 11. b) were mostly 'lower' comparing to the intact curves (Figure 11. a). However, Specimen 16 (green line) was the only one that did not shift its curve from a visual perspective. Specimen 11 (yellow line) had a strange 'larger' curve in the intact group (Figure 11. c). Nevertheless, not much difference can be detected from the 30G group (Figure 11. C and d) for the majority of the curves.

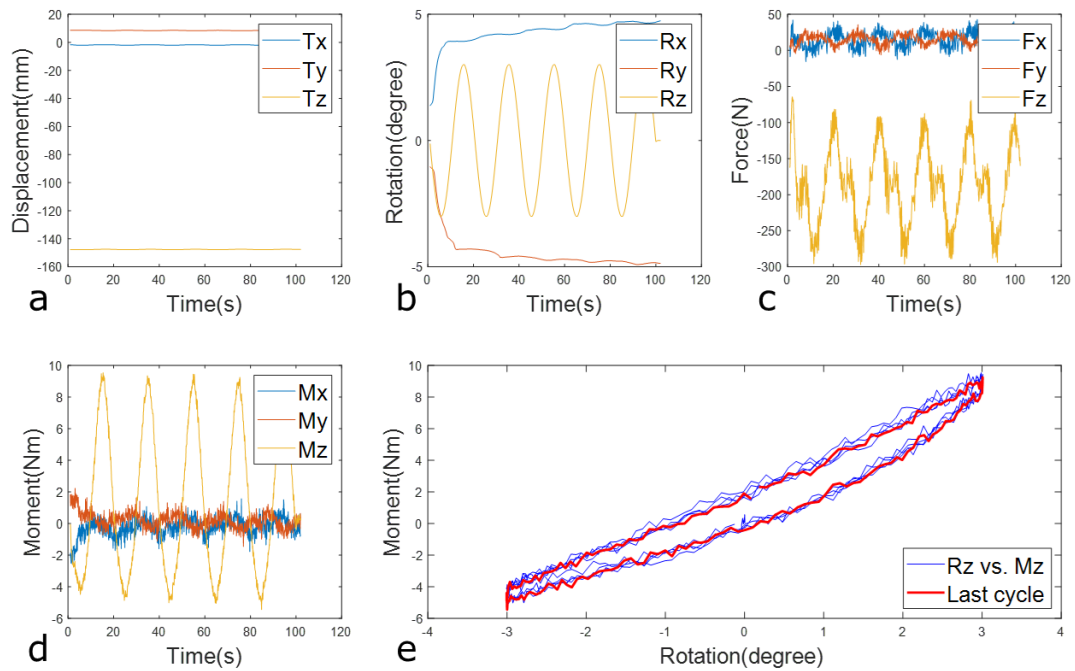


Figure 12. Example of raw 6DOF testing data of $\pm 3^\circ$ axial rotation test applied to a typical FSU specimen. Displacements (a), rotations (b), forces (c), moments (d), and moment-rotation (e) for a representative specimen that underwent testing at a sinewave frequency of 0.05 Hz. All cycles are shown (e) with the final cycle (red line) used for data analysis.

Similarly, a general plot of raw 6DOF testing data of $\pm 3^\circ$ axial rotation test of one typical specimen (Figure 12.). Displacement, rotation, force, moment, and rotation-moment curve was plotted.

No difference can be visually detected from the last cycle curves of lateral bending tests after smoothing of each specimen before and after 25G or 30G needle injury (Figure 13.).

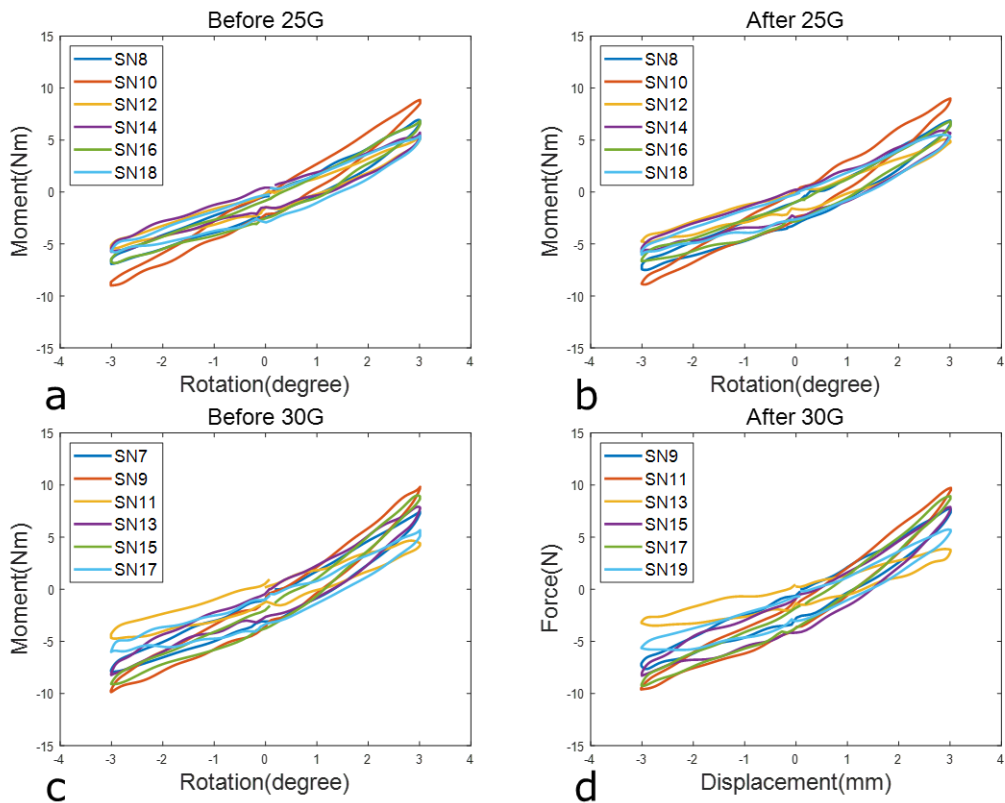


Figure 13. Comparison of last cycle before and after 25G or 30G needle puncture injury of axial rotation tests. (a) Before 25G needle injury, (b) After 25G needle injury, (c) Before 30G needle injury, (d) After 30G needle injury. Legend identifies specimen ID numbers.

Similarly, a general plot of one typical specimen of how displacements, rotations, forces, and moments change over time, and a rotation vs. moment curve of $\pm 3^\circ$ flexion and extension test (Figure 14.). Unlike the previous lateral bending and axial rotation tests, the flexion and extension test does not have too much useful information on stiffness and hysteresis zeroed loss area because of the giant noise and meaningless curve (Figure 14. e). Also, a negative value would come up if calculating the right stiffness. Hence, the author decided to not include the comparison of last cycle and biomechanical properties calculations for flexion and extension since it does not provide comparable information. Hence, there is no stiffness, hysteresis loss area/coefficient, or phase angle are present in the Tables in the discussion.

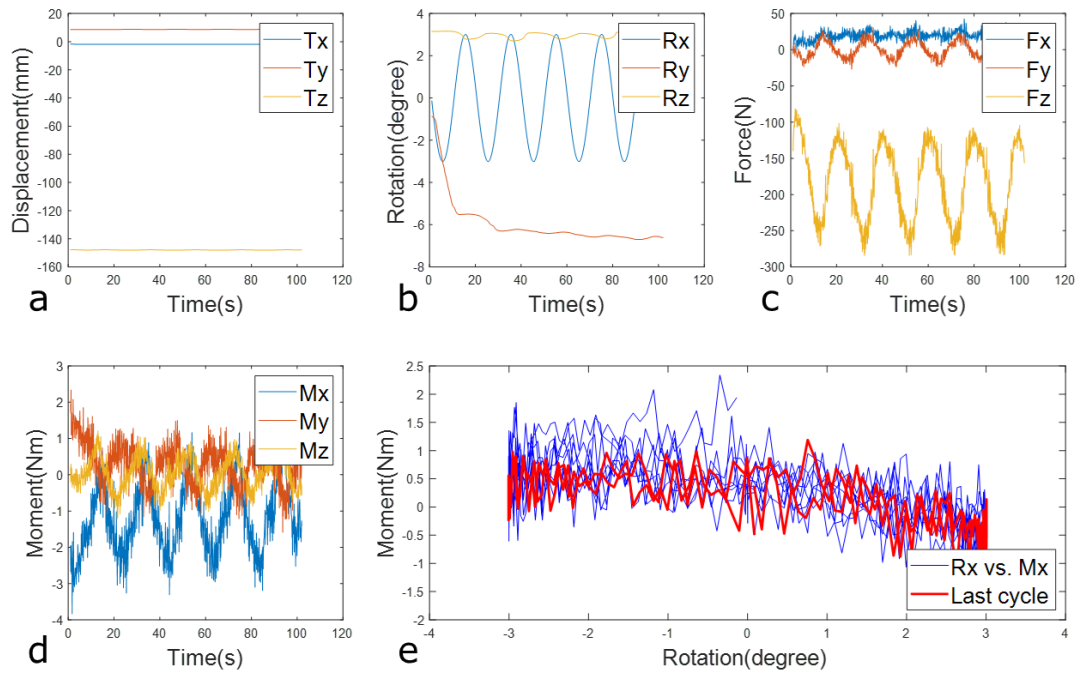


Figure 14. Example of raw 6DOF testing data of 3° flexion-extension test applied to a typical FSU specimen. Displacement (a), rotations (b), forces (c), moments (d), and moment-rotation (e) for a representative specimen that underwent testing at a sinewave frequency of 0.05 Hz. All cycles are shown (e) with the final cycle (red line) used for data analysis.

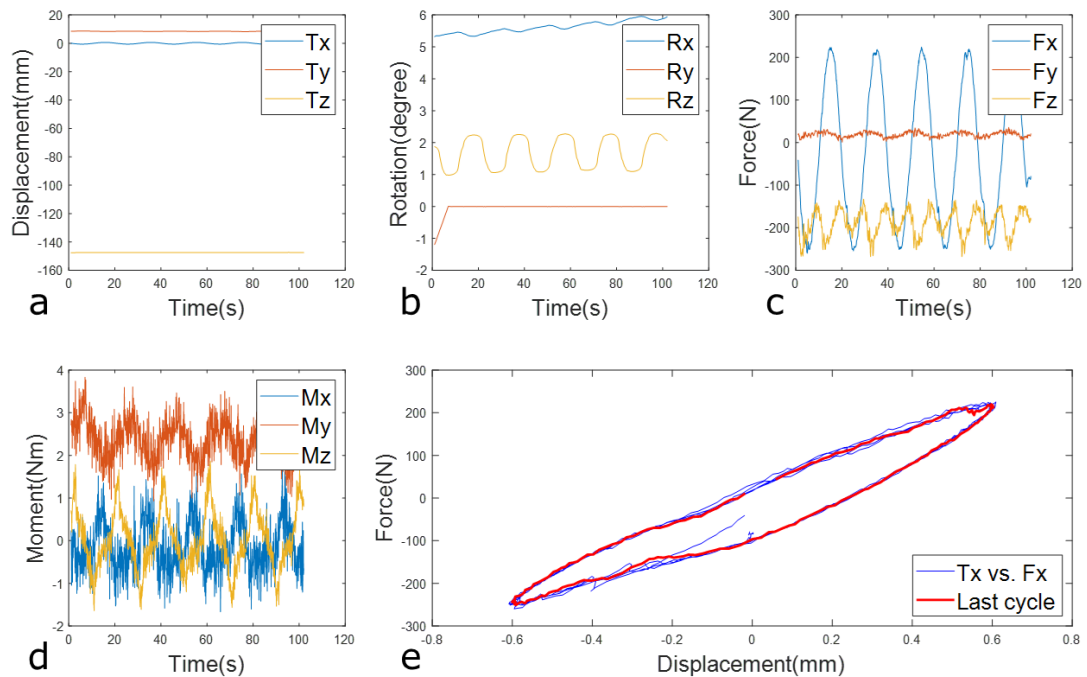


Figure 15. Example of raw 6DOF testing data of 0.6mm left-right lateral shear test applied to a typical FSU specimen. Displacement (a), rotations (b), forces (c),

moments (d), and moment-rotation (e) for a representative specimen that underwent testing at a sinewave frequency of 0.05 Hz. All cycles are shown (e) with the final cycle (red line) used for data analysis.

Still using one typical specimen as the example, unlike the previous three rotational tests, this is a shear test refer to displacement on x-axis and the displacement goes both negative and positive (Left and right) direction. The blue line (Figure 15. a) indicates the cyclic displacement input on x-axis, it is hard to distinguish as the magnitude was only 0.6mm. It is easy to obtain that there are also cyclic rotation and force inputs on y and z-axis which are the position-load control function trying to maintain the 'static condition' of y and z-axis (Figure 15. b, c). Displacement vs. force curve of a $\pm 0.6\text{mm}$ left and right lateral test with a frequency of 0.05Hz was plotted (Figure 15. e), and the last cycle was highlighted (red line). Less noise is obtained comparing to the rotational curves as expected because the force has a much larger magnitude than moment which makes the noise relatively 'smaller'. The last cycle of each specimen from before and after 25G and 30G was plotted and no difference can be visually detected (Figure 16.). It is worth mention that, there is some disparity in the curves if comparing the two intact group (Figure 16. a, c).

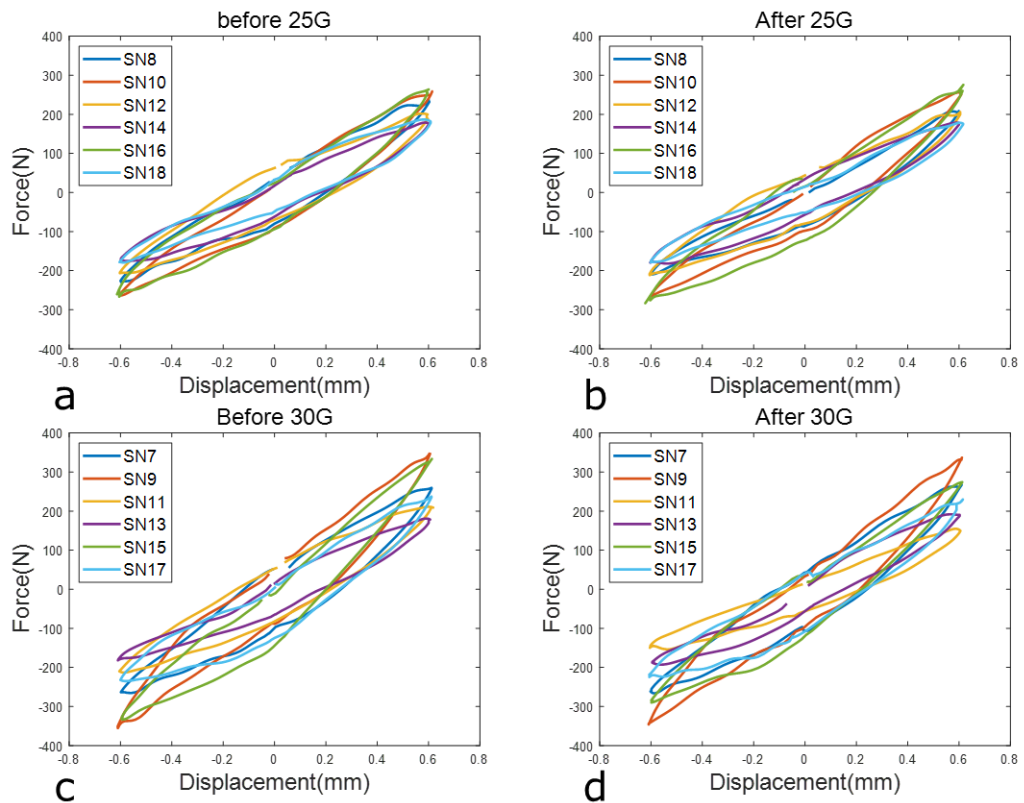


Figure 16. Comparison of last cycle before and after 25G or 30G needle puncture injury of left and right lateral shear tests. (a) Before 25G needle injury, (b) After 25G needle injury, (c) Before 30G needle injury, (d) After 30G needle injury. Legend identifies specimen ID numbers.

The displacement, rotation, force, moment, and displacement vs. force curves of anterior and posterior shear test all plotted (Figure 17). The orange line indicates the shear displacement on y-axis of $\pm 0.6\text{mm}$ with a frequency of 0.05Hz (Figure 17. a). Similarly, the raw data plot of displacement vs. force was plotted (Figure 17. e) and the last cycle been choosing is highlighted (red line).

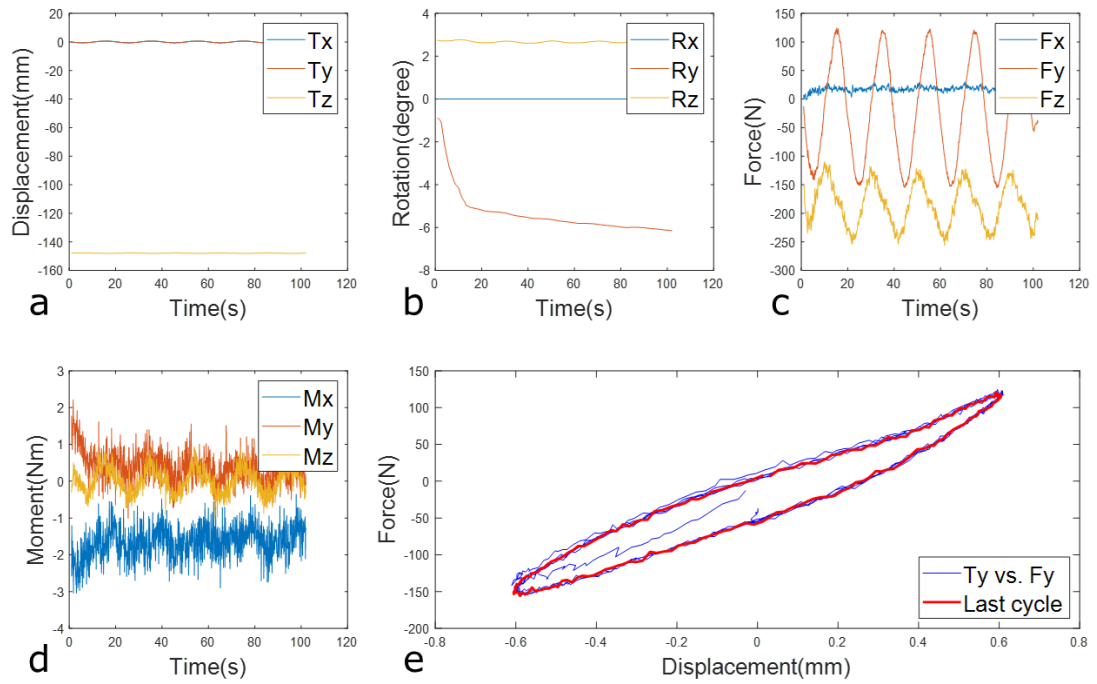


Figure 17. Example of raw 6DOF testing data of 0.6mm anterior-posterior shear test applied to a typical FSU specimen. Displacement (a), rotations (b), forces (c), moments (d), and moment-rotation (e) for a representative specimen that underwent testing at a sinewave frequency of 0.05 Hz. All cycles are shown (e) with the final cycle (red line) used for data analysis.

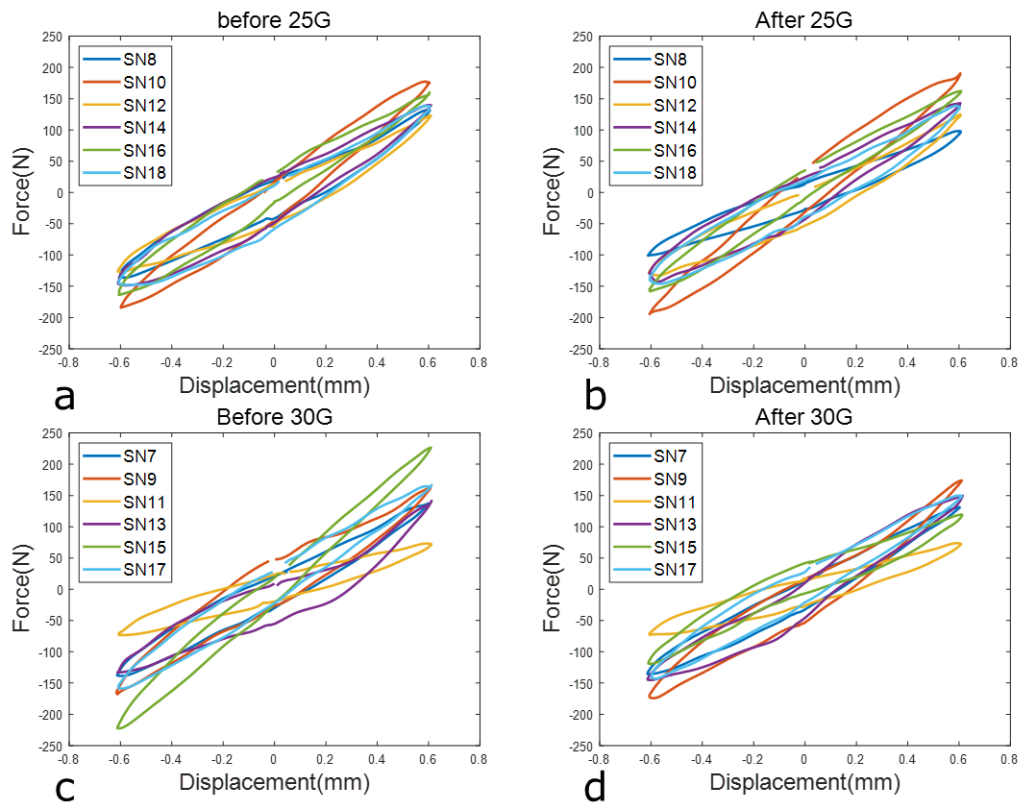


Figure 18. Comparison of last cycle before and after 25G or 30G needle puncture injury of left and right lateral shear tests. (a) Before 25G needle injury, (b) After 25G needle injury, (c) Before 30G needle injury, (d) After 30G needle injury. Legend identifies specimen ID numbers.

It is hard to obtain whether there is a significant difference between before and after needle injury for both groups (Figure 18). More disparity of the curve was found in the intact 30G needle injury group (Figure 18. c), and specimen 11 (yellow line) seems to remain unchanged after needle injury.

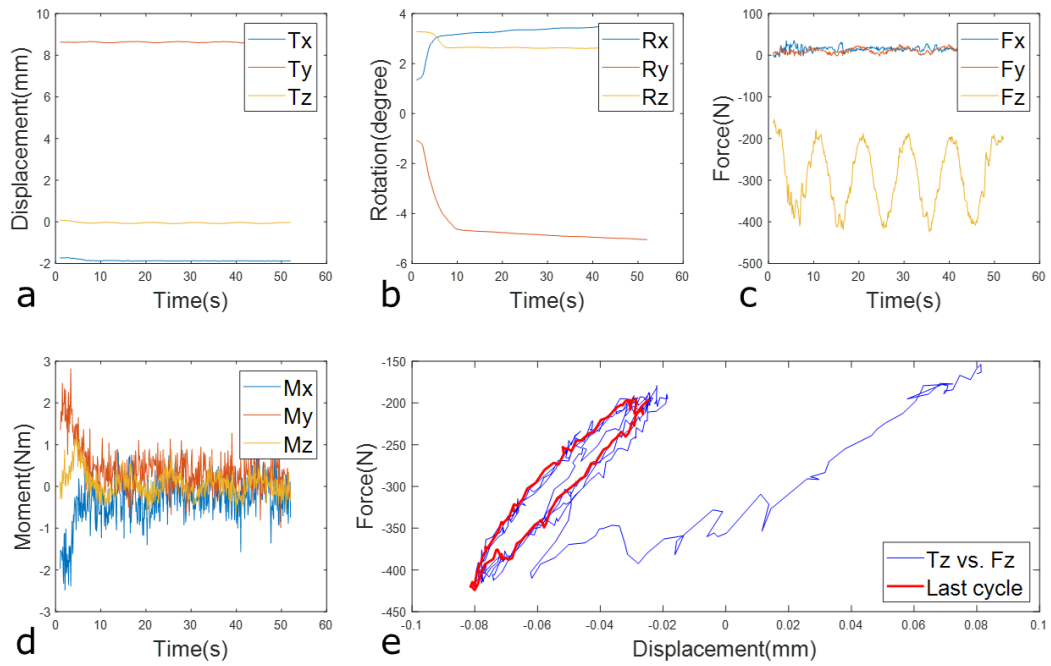


Figure 19. Example of raw 6DOF testing data of compression tests applied to a typical FSU specimen. Displacement (a), rotations (b), forces (c), moments (d), and moment-rotation (e) for a representative specimen that underwent testing at a sinewave frequency of 0.05 Hz. All cycles are shown (e) with the final cycle (red line) used for data analysis.

Raw data of the compression test with a cyclic negative force (Figure 19 c, yellow line) was plotted (Figure 19). The upper and lower limits of the displacement were very small (0.06mm) the curve of displacement vs. force was very noisy (Figure 19. e). Combine the force plot (Figure 19. c) and displacement vs. force plot (Figure 19. e), unlike the former tests and graphs, it is found that the starting and finishing stage of compression test is very noisy.

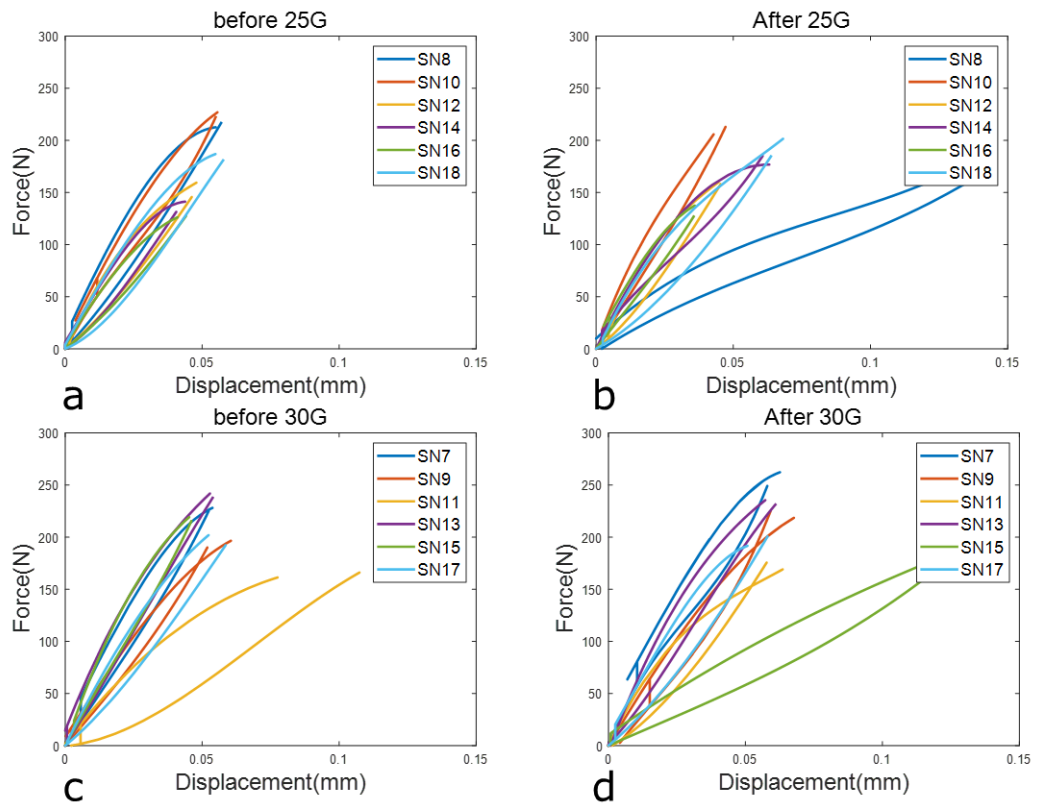


Figure 20. Comparison of last cycle before and after 25G or 30G needle puncture injury of compression tests. (a) Before 25G needle injury, (b) After 25G needle injury, (c) Before 30G needle injury, (d) After 30G needle injury. Legend identifies specimen ID numbers.

Specimen 8 (blue line) after 25G needle injury (Figure 20. b) and, specimen 11 (yellow line) before 30G needle injury (Figure 20. c) and specimen 15 (green line) after 30G needle injury (Figure 20. d) can all be treated as ‘error’ and reject when performing data analysis due to their shapes. The displacement was very small in the compression test which makes it even harder to analysis.

As concluded after each plot, it is very hard to check whether there is a significant difference between before and after needle injury, and some specimens have disparity comparing to others.

5.2 Stiffness

Table 1. Averaged 'positive region' and 'negative region' stiffness of each DOF with standard deviation. The unit of lateral shear, anterior-posterior shear, and compression is N/mm; The unit of axial rotation, lateral bending, and flexion-extension is Nm/°.

	Stiffness region	Before 25G	After 25G	Before 30G	After 30G
Left and Right Lateral Shear (SD)	Right	276 (72)	298 (77)	336 (109)	330 (102)
	Left	232 (65)	204 (57)	244 (119)	220 (121)
Anterior-Posterior shear (SD)	Anterior	218 (22)	194 (25)	231 (91)	184 (76)
	Posterior	147 (49)	157 (38)	193 (81)	154 (60)
Compression (SD)	Compressive	3362 (383)	3371 (609)	4029 (497)	3602 (331)
Axial rotation (SD)	Right	2.3 (0.6)	2.4 (0.5)	2.9 (1.0)	3.0 (1.0)
	Left	1.5 (0.5)	1.3 (0.5)	1.5 (0.7)	1.3 (0.8)
Lateral bending (SD)	Right	0.7 (0.2)	0.9 (0.3)	1.1 (0.2)	1.2 (0.2)
	Left	0.8 (0.4)	0.8 (0.3)	0.9 (0.3)	0.9 (0.6)
Flexion-Extension (SD)	NA	NA	NA	NA	NA

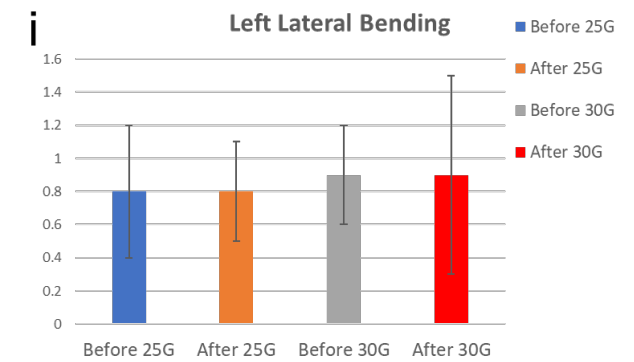
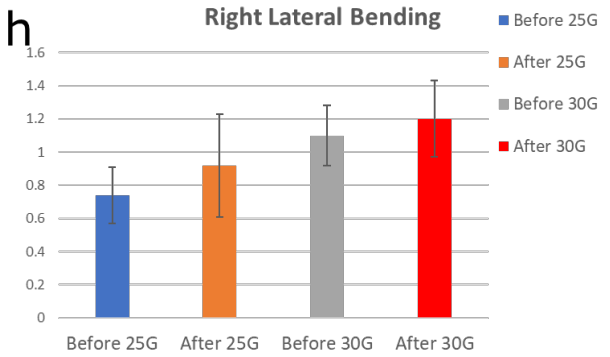
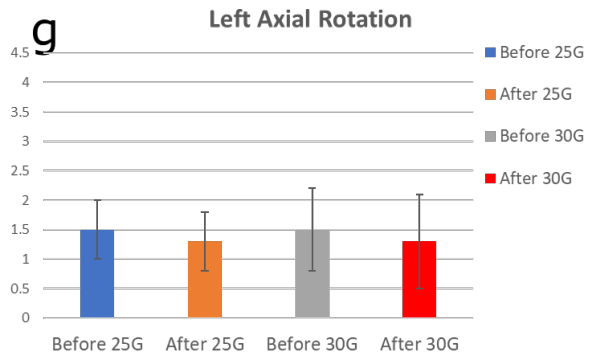
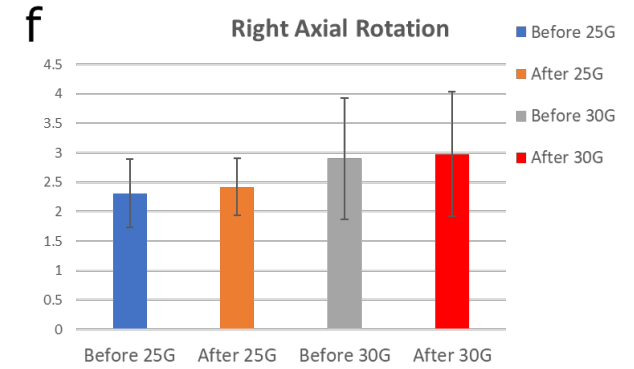
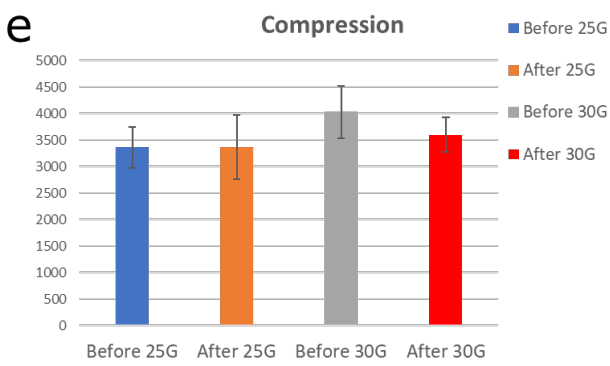
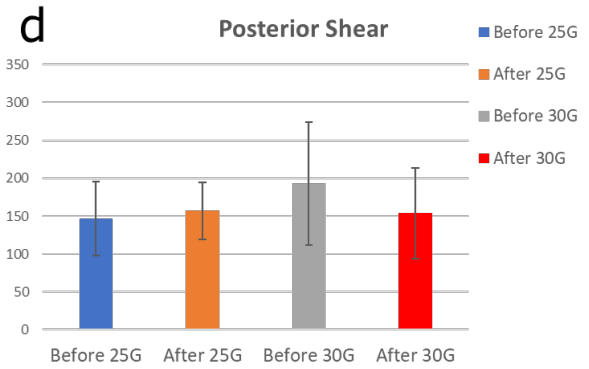
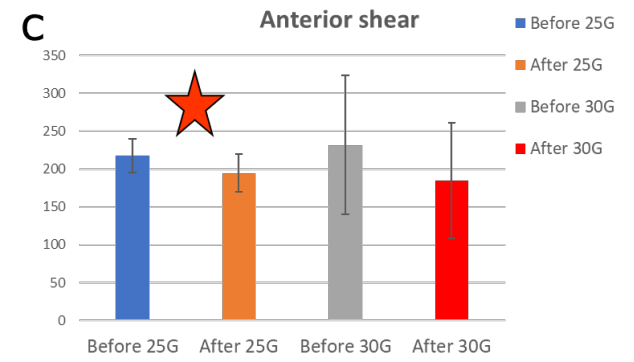
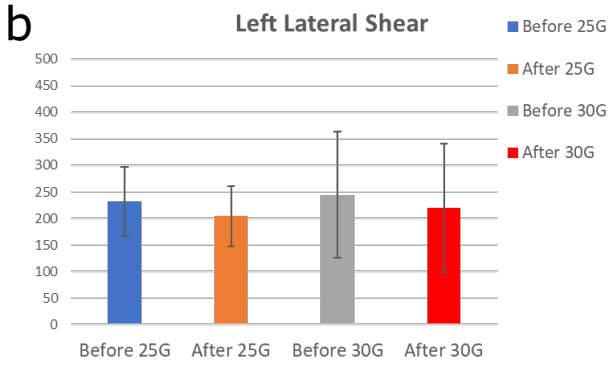
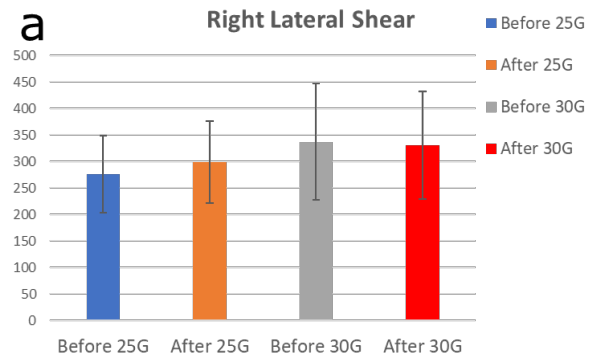


Figure 21. Bar chart showing the averaged stiffness of each DOF except for flexion-extension, taken from Table 1. (a) Right Lateral shear; (b) Left lateral shear; (c) Anterior shear; (d) Posterior shear; (e) Compression; (f) Right Axial Rotation; (g) Left Axial Rotation; (h) Right Lateral Bending; (i) Left Lateral Bending.

After conducting t-tests on each group each DOF, only anterior stiffness test (Figure 21. c, Red star) has a significant difference ($p = 0.048$) due to the 25G needle injury (See [Appendix F](#)). The stiffness in other DOFs also have changed due to the needle injury but those differences are not significant and have no pattern to conclude.

Significant differences were found when comparing the 'positive region' stiffness and 'negative region' stiffness from same group. Theoretically, the 'positive region' stiffness and 'negative region' stiffness should be similar, because they were calculated from the same specimen. However, the left and right stiffnesses of lateral shear test before (grey bar in Figure 21. a and b) and after (red bar in Figure 21. a and b.) showed a disparity of about 30%. Similar situation was also found in 30G group of axial rotation test (grey and red bar in Figure 21. f and g). Besides, standard deviation was also found quite big in the 30G group lateral shear test.

5.3 Hysteresis zeroed loss area and coefficient

Table 2 Averaged Hysteresis loss area of each group before and after needle injury of each DOF. The unit is Jules.

	Before 25G	After 25G	Before 30G	After 30G
Left and Right Lateral Shear (SD)	96 (15)	96 (24)	114 (24)	104 (30)
Anterior-Posterior shear (SD)	58 (7)	52 (9)	49 (8)	48 (6)
Compression (SD)	1.6 (0.6)	1.3 (0.6)	1.41 (0.5)	1.6 (0.5)
Axial rotation (SD)	9.8 (1.4)	10.6 (1.9)	11.3 (1.6)	11.5 (2.2)
Lateral bending (SD)	11.4 (2)	12.2 (2.5)	14.3 (5.1)	12.7 (3.1)
Flexion-Extension (SD)	NA	NA	NA	NA

Table 3 Averaged Hysteresis loss coefficient of each group before and after needle injury of each DOF. No unit.

	Before 25G	After 25G	Before 30G	After 30G
Left and Right Lateral Shear (SD)	0.56 (0.02)	0.54 (0.03)	0.57 (0.02)	0.55 (0.03)
Anterior-Posterior shear (SD)	0.5 (0.03)	0.47 (0.03)	0.48 (0.04)	0.46 (0.02)
Compression (SD)	0.25 (0.03)	0.25 (0.04)	0.24 (0.04)	0.24 (0.05)

Axial rotation (SD)	0.40 (0.02)	0.42 (0.02)	0.42 (0.02)	0.43 (0.02)
Lateral bending (SD)	0.77 (0.03)	0.80 (0.03)	0.66 (0.03)	0.70 (0.05)
Flexion-Extension (SD)	NA	NA	NA	NA

There was no significant difference comparing before and after needle injury in both 25G and 30G group (See [Appendix F](#)). No particular pattern of decreasing or increasing can be found in both groups. It was found that lateral shear tests resulted in the biggest hysteresis loss area, followed with anterior-posterior shear, compression test has the smallest energy absorption (Table 2). It is consistent in hysteresis loss are coefficient where compression has the lowest percentage among the three displacement control tests.

Axial rotation and lateral bending tests had similar hysteresis loss area (Table 2.), but lateral bending had a higher hysteresis loss coefficient (Table 3.). In general, the data of hysteresis loss area and hysteresis loss coefficient supported each other.

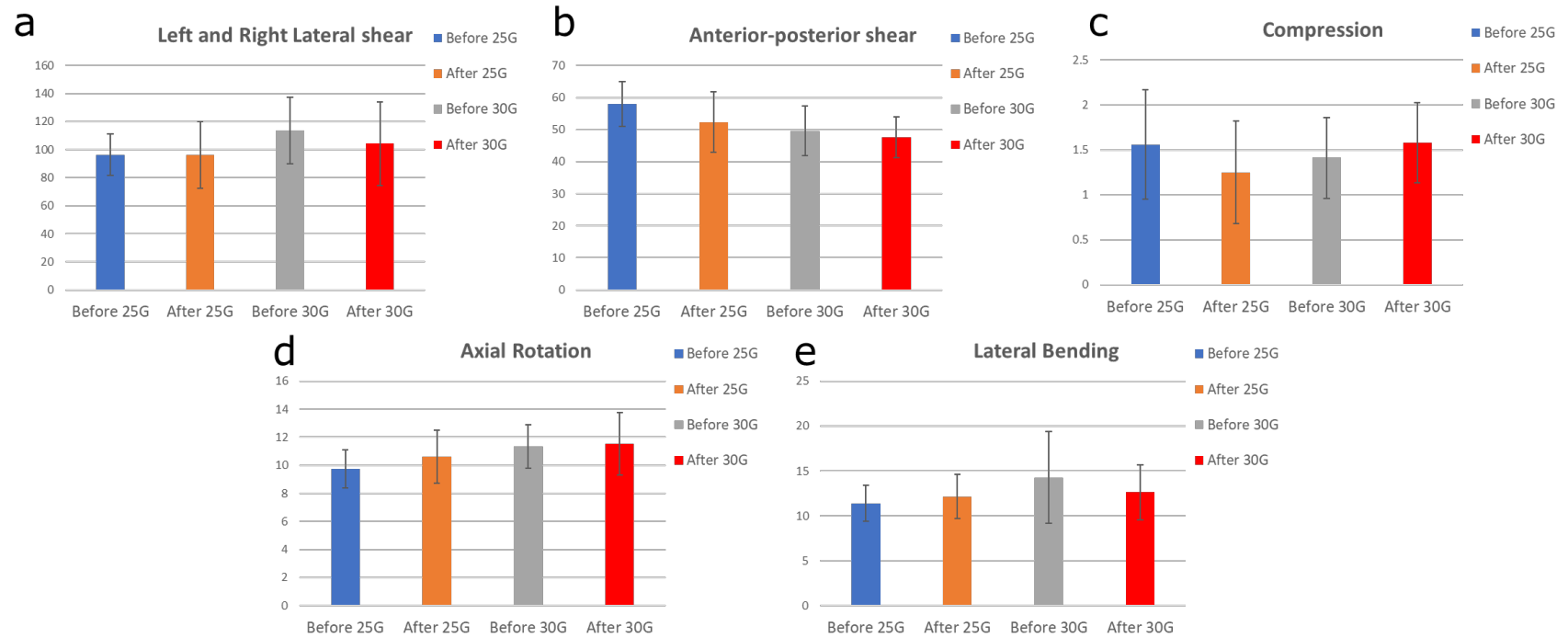


Figure 22 Bar chart showing the Averaged hysteresis loss area of each DOF with SD except for flexion-extension. (a) Left and Right Lateral shear; (b) Anterior-posterior shear; (c) Compression; (d) Axial rotation; (e) Lateral bending.

5.4 Phase angle

Table 4 Averaged Phase Angle of each group before and after needle injury of each DOF. The unit is °.

	Before 25G	After 25G	Before 30G	After 30G
Left and Right Lateral Shear	12.6 (1.5)	12.5 (2.1)	12.77 (2.2)	12 (1.8)
Anterior-Posterior shear	11.2 (2.1)	10.4 (1.8)	10.4 (3.3)	10.4 (2.2)
Compression	13.7 (2.3)	12.5 (1.8)	11.2 (1.7)	14.3 (3.7)
Axial rotation	9.2 (2.0)	9.8 (2.4)	9.9 (3.4)	10.1 (3.7)
Lateral bending	18 (4.1)	18.1 (3.8)	16 (2.8)	16.7 (3.4)
Flexion-Extension	NA	NA	NA	NA

There is no significant difference is found when comparing before and after needle injury in both 25G and 30G group (See [Appendix F](#)). Lateral bending has the highest phase angle while axial rotation has the lowest among all DOFs (Table 4.).

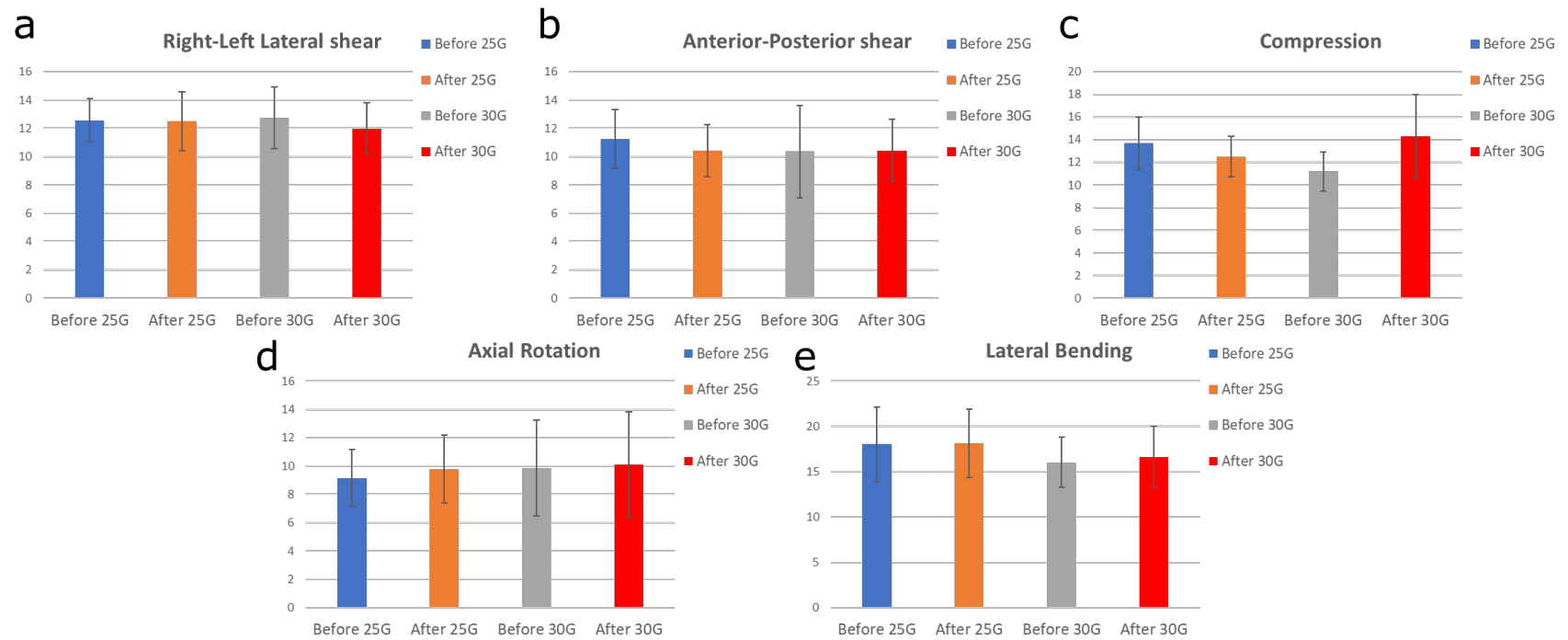


Figure 23 Bar chart showing the Averaged phase angle of each DOF with SD except for flexion-extension. (a) Left and Right Lateral shear; (b) Anterior-posterior shear; (c) Compression; (d) Axial rotation; (e) Lateral bending.

5.5 Overnight preload comparison

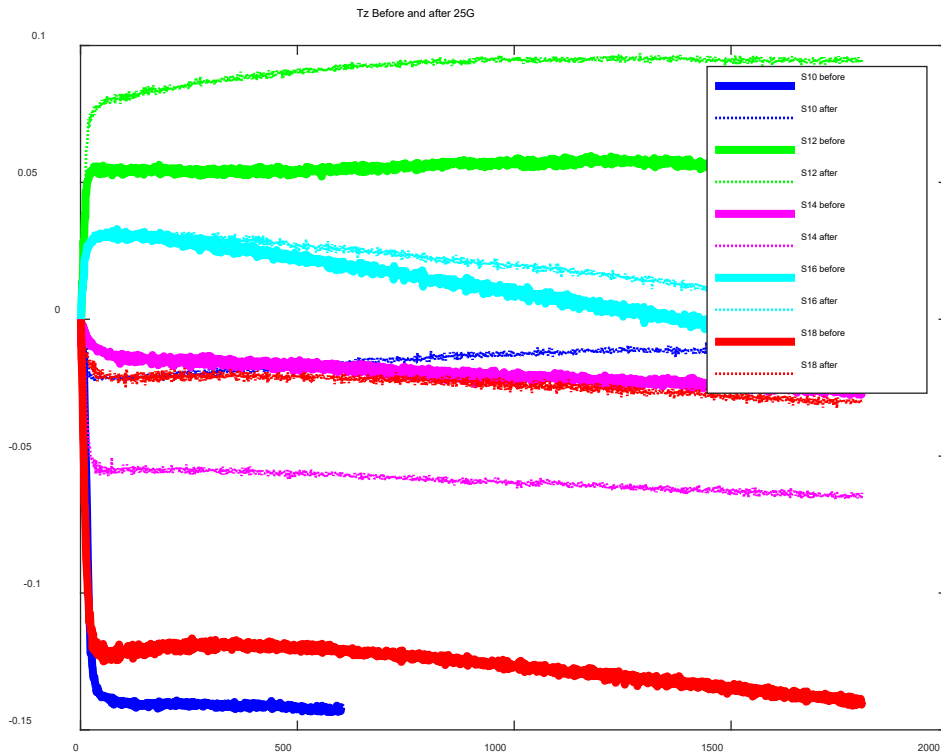


Figure 24 Displacement over time of 25G needle injury group overnight compressive preload. Specimen data before and after needle injury is plotted in the same color, the thick solid line represents the intact data, the dotted thin line represents the injured data.

The author also plotted displacement over time of 30G group, and force over time of both 25G and 30G group, but those curves do not provide useful comparable information (See [Appendix G](#)). From the plot, it is obvious that all the specimens were reaching steady-state and there is a different deformation between before and after needle injury.

Chapter 6. Discussion

The final project was mainly focused on the analysis of previous experimental data. The proposed project was designed to investigate how different needle injury levels and fatigue affect the 6DOF biomechanics and failure properties. However, COVID-19 started just before lab experiment stage. Unfortunately, the scope of the project had to shift to data analysis. The data analysing methods and skills are still applicable and helpful for finishing the proposed project and future study. Data analysis on how 25G and 30G needle injury affect the stiffness and energy absorption was performed. Unlike to the proposed project plan (7% and 40% of averaged disc height), two relatively small needles (6.2% and 10.2% of averaged disc height) were used in the previous experimental tests.

The 'positive region' and 'negative region' stiffness, hysteresis loss area/coefficient, and phase angle of the sheep lumbar disc were assessed both before and after needle injury. The quantitative assessments were taken in each DOF except for flexion-extension due to its very noisy curve which would provide little useful information. Only anterior-posterior shear stiffness has been obtained a significant drop after 25G needle injury. Stiffness in other DOFs are not obtained any significant changes after evaluating with t-Test. Similarly, no significant difference was found in terms of hysteresis zeroed loss area/coefficient or phase angle in every DOF. Thus, no acute effect was obtained in 6DOF biomechanics in this sheep lumbar disc experiment after the needle injury except for posterior-anterior shear stiffness. Besides, no particular pattern of decrease or increase can be found from the plots of displacement or force over time of the overnight compressive loading even though with some very small variations.

The expected stiffness decreases only showed up in anterior-posterior shear test after 25G needle injury, and even no change was found in the hysteresis loss area and phase angle. It is interesting that, in 30G group, some increases were obtained in the axial rotation and lateral bending stiffness (see Figure 21. d-e). Because of the very small numbers that rotational stiffness got with the consideration of the accuracy of linear regression and slope calculation, those very small increases are acceptable. For hysteresis zeroed loss area and phase angle, their results were

supporting each other since no significant difference was found for both. No particular rising or dropping trend can be obtained due to needle injury.

Based on author's knowledge, the disc itself mainly withstand the compressive load of upper body with the jelly-like material inside the nucleus pulposus in human spine and this also applied in sheep model. The annulus fibrosus is the structure that responds to minor shear force or displacement. There should be a decrease in both axial and rotational stiffness as hypothesis due to the fluid leakage inside nucleus pulposus and structural damage of the annulus fibrosus as the results of the needle injury. Studies have suggested that the severity of acceleration of disc degeneration due to needle injury is based on the needle diameter^{10,14}. Although a needle diameter of 40% of disc height was suggested by Elliott, et al. as the threshold of whether there are universal changes of disc. Still, there are also researchers have found that there will be an acute effect in terms of disc's biomechanics even with a very small needle (10% of disc height)^{10,45}. Rotational stiffness which governed by the annulus fibrosus is suggested to change with increasing needle size⁴. However, the rotational stiffness is obtained with no significant difference after needle injury which is not consistent with previous study. Acute effect in axial stiffness was only been found in anterior-posterior shear test after 25G needle puncture, which is partly consistent with the previous needle size-related theory of axial biomechanics⁵⁰.

It is found that, the t-test results of hysteresis loss area/coefficient remain consistent when comparing to phase angle's p-value. A larger phase angle means a bigger interval between the input (displacement or rotation) and output (force or moment) which also gives insight into the viscoelasticity of the disc, a larger hysteresis zeroed loss area indicates bigger energy absorption. These two should have the same trend in theory, as higher energy absorption is a sign of increasing viscoelasticity.

For the figure of displacement or force over time of the overnight compressive load (Figure 25. and [Appendix G](#)), a steady-state of displacement was eventually reached for both groups as they are simulating the disc resting of overnight sleep. The data was zeroed for better comparison. In theory, negative numbers of displacement are expected with a compressive load applying on the disc. However, Specimen 12

(Green) and Specimen 16 (Light blue) showed positive displacement while reaching the steady state. A very small value of displacement (around ± 0.1 mm) was obtained from the overnight compressive loading graph, considering the accuracy of the machine, the very small positive number can be acceptable. On the other hand, changes were obtained after 25G needle injury but no specific trend in increasing or decreasing can be concluded with such small numbers.

These results were consistent with the previous studies which induced needle puncture (needle diameter less than 25% of the disc height) into the discs with different animal models. No acute effect on biomechanics, disc height, or other biochemical assessment, such as the Glycosaminoglycan (GAG) content was found when using needles less than 25% of the disc height with or without actual contrast agent being injected into the disc^{10,51,52}. In this project, 25G (10.2% of disc height) and 30G (6.2% of disc height) needle were used to induce the needle injury, and their diameters were very small and far away from 25%. However, if looking at the magnitude of the stiffness values, the axial stiffness obtained in this project is larger than those present in previous studies. This may be because of the stiffness measuring region difference. This study calculated the stiffness from the linear region instead of the neutral zone. With Flinders Hexapod machine, tests were all under hybrid position-load control, unlike the others who use stepwise loading or ramp loading. Hence, higher accuracy is achieved.

What's more, it is known that the spinal level of disc plays an important role in the disc degeneration as lower levels come with higher possibility of disc degeneration due to the higher load they withstand. The discs being used in the experiment are mainly L3-4 with several L2-3. Ideally, a consistence in specimens should be achieved to maximize the variable control method. However, this study does not specifically focus on one level. Still, to make them easy to compare, all specimens have a very close diameter and height.

Some limitations were exposed during the data analysing. Firstly, the 30G group may not have a very consistent mechanical property as obtained (Figure 20. a-d), a relatively high standard deviation in each grey bar. This means that some differences already exist before introducing needle injury into the discs. However, this might be

the reason for increasing stiffness in some DOFs after 30G needle injury. Secondly, the posterior elements were removed during specimen preparation to make sure that the experiment only focuses on the disc itself. However, this will make the result not clinically relevant. Thirdly, from the comparison plot, it is obvious that some of the data is not useful as they are unacceptably out of the normal region (Figure 20). Besides, how to or whether it is possible to use the flexion-extension data remains unclear. All animal models have their strengths and limitations. In this project, sheep lumbar spine is chosen as the specimens due to its very similar geometric parameters and disc height and area data after normalizing comparing to human. However, if looking at the torsion parameters, even after geometric normalization, sheep was still statistically different from human⁹. Still, some trade-off must be made on every aspect in the experiment design, it is impossible to find a very best specimen that fits every demand to work with.

Chapter 7. Conclusion

The biomechanical properties of sheep lumbar discs were successfully assessed in terms of stiffness, hysteresis zeroed loss area, and phase under all 6DOF hybrid position-load control before and after two different sizes of needle. Codes of data analysis using MATLAB was developed and statistical analysis of the biomechanics were performed. Averaged stiffness was found no significant difference before and after both 25G and 30G needle injury in all 6DOF apart from anterior-posterior shear. A decreasing trend was obtained in the anterior-posterior shear stiffness after 25G needle injury. The same condition was found in both hysteresis loss area and phase angle with a result of no significant difference due to the needle injury. Furthermore, the plots of displacement and force over time of the overnight compressive load were also analysed and no particular trend in decreasing or increasing of the deformation can be concluded.

Future work is needed to perform the already designed experiment to investigate how clinical sized needle and needle with 40% of disc height, and fatigue (simulating one-day human labour activities) affect the 6DOF and failure biomechanics of the discs with the acquired data analysing and statistic analysing skills from this project. Due to the COVID-19, we have to delay the original project design and shift the focus into previous experimental data analysing. Also, other mechanical parameters, such as the range of motion, the neutral zone stiffness, disc height after needle injury etc. can also be investigated and analysed as part of the future work since all these biomechanical properties are important criteria in disc degeneration assessment.

Whether keep the posterior elements of the FSU or not is always a debate, as keeping it will make the experiment clinically relevant, but it will affect the results if the experiment designs to investigate the disc biomechanics. Hence, to solve this, another experiment design that focuses on how posterior elements affect the disc's biomechanics might be needed.

Appendices

Appendix A Table of literature review summary

Title	Author/date	Methods	Findings
A novel rabbit model of mild, reproducible disc degeneration by anulus needle puncture: correlation between the degree of disc injury and radiological and histological appearances of disc degeneration	Masuda, K., Aota, Y., Muehleman, C., Imai, Y., Okuma, M., Thonar, E. J., ... & An, H. S. (2005)	<ul style="list-style-type: none"> - The classic annular stab model and the new needle puncture model were used in the rabbit (N=26). - For the needle puncture model, 3 different gauges of needle (16G, 18G, and 21G) were used to induce an injury to the disc to a depth of 5 mm. - Radiographic and histologic analyses were performed; magnetic resonance images were also assessed in the needle puncture model. 	<ul style="list-style-type: none"> - The needle puncture approach, using 16G to 21G needles, resulted in a reproducible decrease of disc height and magnetic resonance imaging grade. - The ease of the procedure and the transfer of the methodology (anulus needle procedure) will benefit researchers studying disc degeneration.
Needle puncture injury affects intervertebral disc mechanics and biology in an organ culture model	Korecki, C. L., Costi, J. J., & Iatridis, J. C. (2008).	<ul style="list-style-type: none"> - Bovine caudal intervertebral discs were harvested, punctured posterolaterally using 25G and 14G needles, and placed in organ culture for 6 days (n = 10). - Discs underwent a daily dynamic compression loading protocol for 5 days from 0.2 to 1 MPa at 1 Hz for 1 hour. - Disc structure and function were assessed with measurements of dynamic modulus, creep, height loss, water content, proteoglycan loss to the culture medium, cell viability, and histology. 	<ul style="list-style-type: none"> - Needle puncture injury caused a rapid decrease in dynamic modulus and increase in creep during 1-hour loading, although no changes were detected in water content, disc height, or proteoglycan lost to the media. - Relatively minor disruption in the disc from needle puncture injury had immediate and progressive mechanical and biologic consequences with important implications for the use of discography, and repair-regeneration techniques.

<p>The effect of relative needle diameter in puncture and sham injection animal models of degeneration</p>	<p>Elliott, D. M., Yerramalli, C. S., Beckstein, J. C., Boxberger, J. I., Johannessen, W., & Vresilovic, E. J. (2008)</p>	<ul style="list-style-type: none"> - Mechanics were measured after sham phosphate buffered saline injection with a 27 G or 33 G needle in the rat and with a 27 G needle in the sheep. - Axial compression-tension cyclic testing was performed; Twenty cycles from 4° were applied at 0.5 Hz with the 400 N compression load maintained. - Twenty-three in vivo studies in the rat, rabbit, dog, or sheep were reviewed. 	<ul style="list-style-type: none"> - When the rat was injected with a 27 G needle (52% of disc height), the compression, tension, and neutral zone stiffnesses were 20% to 60% below preinjected values and the neutral zone length was 130% higher; when injected with a 33 G needle (26% of disc height), the only affected property was the neutral zone length, which was only 20% greater. - When the sheep was injected with a 27 G needle (10% of disc height), none of the axial properties were different from intact, the torsion stiffness was not different, and the torque range was 15% smaller. - Needle size of 40% of disc height is the threshold of whether there is significant disc changes.
<p>Does discography cause accelerated progression of degeneration changes in the lumbar disc</p>	<p>Carragee, E. J., Don, A. S., Hurwitz, E. L., Cuellar, J. M., Carrino, J., & Herzog, R. (2009)</p>	<ul style="list-style-type: none"> - Seventy-five subjects without serious low back pain illness underwent a protocol MRI and an L3/4, L4/5, and L5/S1 discography examination in 1997 (n = 50) with a matched group (n = 52). - subjects were followed for 10 years. - MRI graders, blind to group designation, scored both groups for qualitative findings (Pfirrmann grade, herniations, endplate changes, and high intensity zone). Loss of disc height and loss of disc signal were measured by quantitative methods. 	<ul style="list-style-type: none"> - In all graded or measured parameters, discs that had been exposed to puncture and injection had greater progression of degenerative findings compared to control (noninjected) discs - New disc herniations were disproportionately found on the side of the annular puncture. - The quantitative measures of disc height and disc signal also showed significantly greater loss of disc height (p = 0.05) and signal intensity (p = 0.001) in the discography disc compared to the control disc.

<p>The effect of needle size inducing degeneration in the rat caudal disc: evaluation using radiograph, magnetic resonance imaging, histology, and immunohistochemistry</p>	<p>Keorochana, G., Johnson, J. S., Taghavi, C. E., Liao, J. C., Lee, K. B., Yoo, J. H., ... & Wang, J. C. (2010)</p>	<p>- Lewis rat (n = 36). All rats were divided into three groups according to different needle gauges (18G, 20G, and 22G). Caudal discs were punctured percutaneously under image guidance. - Radiographs and MRI were obtained at 2 weeks interval until 8 weeks. At each time point, three rats from each group were sacrificed for histological analysis and immunohistochemistry.</p>	<p>- Larger needle gauges, especially 18G, produced more deterioration of the disc when compared with smaller sizes, particularly with time. - For the effect of time in the same needle size, the differences occurred between 2- or 4-week and 8-week time point in the 18G and 20G groups. - The proteoglycan and aggrecan stain gradually decreased over time. Chondrogenic differentiation was identified within the degenerative disc by detecting Sox-9 positive cells and collagen II accumulation increased as degeneration progressed.</p>
<p>Needle puncture injury causes acute and long-term mechanical deficiency in a mouse model of intervertebral disc degeneration</p>	<p>Martin, J. T., Gorth, D. J., Beattie, E. E., Harfe, B. D., Smith, L. J., & Elliott, D. M. (2013).</p>	<p>- Needle puncture injuries were created in the caudal intervertebral discs of mice to induce disc degeneration. Compression, torsion, and creep mechanics were assessed both immediately and after eight weeks to distinguish between the effects of injury and the subsequent reparative or degenerative response. - Two needle sizes (29 and 26 gauge) were used to determine injury size dependence.</p>	<p>- Compressive stiffness (62%), torsional stiffness (60%), and early damping stiffness (84%) decreased immediately after injury with the large needle (26G). These mechanical properties did not change over time despite structural and compositional changes - The small needle size had no significant effect on mechanics and did not initiate degenerative changes in structure and composition. - Thus, the injection of therapeutics into the NP with a minimal needle size may limit damage due to the needle insertion.</p>

Needle puncture in rabbit functional spinal units alters rotational biomechanics	Hartman, R. A., Bell, K. M., Quan, B., Nuzhao, Y., Sowa, G. A., & Kang, J. D. (2015).	<ul style="list-style-type: none"> - Rabbit FSUs were tested using a robot testing system whose force/moment and position precision were assessed to demonstrate system capability. - Destructive testing: load-to-failure (n = 3-5), Non-destructive testing: flexibility testing (n = 8), control (n = 5). - No. 11 blade stab group serves as the positive control (n = 8), 16G needle was inserted on the left side to a 5mm depth using the anterolateral approach (n = 8). 	<ul style="list-style-type: none"> - The key findings are that neutral zone stiffness is reduced and range of motion in flexion/extension is increased due to the needle puncture. Reduced stiffness and hypermobility indicate reduced stability of the FSU following a 16G needle puncture of the disc. - No. 11 blade-stab significantly increased range-of-motion in all motions, decreased neutral zone stiffness and width (N m) in flexion/extension, and increased elastic zone stiffness in flexion and lateral bending.
Effect of needle diameter, type and volume of contrast agent on intervertebral disc degeneration in rats with discography	Huang, X., Wang, W., Meng, Q., Yu, L., Fan, C., Yu, J., ... & Ye, X. (2019).	<ul style="list-style-type: none"> - Three separate experiments examined needle diameter, and type and volume of contrast agent (n = 10). - Coccygeal discs (Co7-10) adult male rats were used. - Group 1: 30G compare to 21G; - Group 2: two different types of contrast agent; - Group 3: 2ul and 3ul of same contrast agent using both 30G needle. - X-rays were used to detect the disc height degeneration index at 1, 2 and 4 weeks after the procedure. - MRI was used to study the changes in the disc structure and the signal intensity of IVD 2 and 4 weeks after the procedure. - Disc water content and histology were measured at 4 weeks after the procedure. 	<ul style="list-style-type: none"> - A 21-g needle significantly increased disc degeneration when compared with the 30-g needle as detected by X-ray, MRI, disc water content and histology (p < 0.05). - Two microlitres of iodine significantly decreased the disc MRI signal and water content at 4 weeks compared with the same volume of normal saline (p < 0.05). - Three microlitres of iodine significantly increased disc degeneration when compared with 2 µl iodine, as detected by X-ray, MRI, disc water content and histology at 4 weeks (p < 0.05). - To reduce disc degeneration after discography, it may be best to choose a smaller needle size, minimize the use of contrast agent and use non-ionic contrast agents with osmotic pressure similar to the intervertebral disc.

Appendix B Code of General plot

```
clear all;

% read the data

P = textread('SN8DB003Rx5E2_P.txt');

L = textread('SN8DB003Rx5E2_L.txt');

Tx = P(1,:);
Ty = P(2,:);
Tz = P(3,:);

Rx = P(4,:);
Ry = P(5,:);
Rz = P(6,:);

Fx = L(1,:);
Fy = L(2,:);
Fz = L(3,:);

Mx = L(4,:);
My = L(5,:);
Mz = L(6,:);

Rxn = Rx * -1;

x=linspace(1,102,1020);

%adjust the figure (by only
moving Rz)

Rx = Rx-(min(Rx)+max(Rx))/2;

Rxn = Rxn-(min(Rxn)+max(Rxn))/2;

% Find the last circle starting &
ending location with Rz and Rxn

[pks,locs] = findpeaks(Rx,'MinPeakDistance',50,'MinPeakHeight',2);

[pks1,locs1] = findpeaks(Rxn,'MinPeakDistance',50,'MinPeakHeight',2);

sp = (locs(end-1)+locs1(end-1))/2; %find the last cycle starting
point

sp = round(sp);

ep = (locs(end)+locs1(end))/2; %find
the last cycle ending point

ep = round(ep);
```

```
RSr = find(Rx(sp:sp+0.25*(ep-
sp))>1.5&Rx(sp:sp+0.25*(ep-
sp))<2.9); %find the right stiffness
```

```
RSr = RSr+sp;
```

```
RSr = round(RSr);
```

```
LSr = find(Rx(sp+0.5*(ep-
sp):sp+0.75*(ep-sp))>-
2.9&Rx(sp+0.5*(ep-
sp):sp+0.75*(ep-sp))<-
1.5); %find the left stiffness
```

```
LSr = LSr+sp+0.5*(ep-sp);
```

```
LSr = round(LSr);
```

```
% Calculate the stiffness
```

```
PR = polyfit(Rx(RSr),Mx(RSr),1);
```

```
RS = PR(1); %right stiffness
```

```
PL = polyfit(Rx(LSr),Mx(LSr),1);
```

```
LS = PL(1); %left stiffness
```

```
% Find the zeroed Hysteresis area
```

```
md = round((sp+ep)/2);
```

```
rq = round(sp+(ep-sp)/4);
```

```
lq = round(ep-(ep-sp)/4);
```

```
prt = polyfit(Rx(sp:rq),Mx(sp:rq),3); %
right
```

```
xrt = Rx(sp:rq); %top
equation
```

```
yrt = polyval(prt,xrt);
```

```
Art = trapz(xrt,yrt);
```

```
prb = polyfit(Rx(rq:md),Mx(rq:md),3);
%bottom equation
```

```
xrb = Rx(rq:md);
```

```
yrb = polyval(prb,xrb);
```

```
Arb = trapz(xrb,yrb);
```

```
Ar = Art+Arb; %
energy absorption at right
```

```
plb = polyfit(Rx(md:lq),Mx(md:lq),3);
%left
```

```
xlb = Rx(md:lq); %bottom
equation
```

```
ylb = polyval(plb,xlb);
```

```
Alb = trapz(xlb,ylb);
```

```

plt = polyfit(Rx(lq:ep),Mx(lq:ep),3); %t
op equation
xlt = Rx(lq:ep);
ylt = polyval(plt,xlt);
Alt = trapz(xlt,ylt);
Al= Alb+Alt; %
energy absorption at left

X = [xrt,xrb,xlb,xlt];
Y = [yrt,yrb,ylb,ylt];

HL = Ar+Al; %Hysteresis
zeroed area

HLc = HL/(Art+Alb); %Hysteresis
zeroed coefficient

% Phase angle
[phi, frq, cxy] = relphase(Rx,Mx);

figure(1)
subplot(2,3,1);
plot(x,Tx,x,Ty,x,Tz);
xlabel('Time(sec)');

ylabel('Displacement(mm)');
legend('Tx','Ty','Tz');
subplot(2,3,2);
plot(x,Rx,x,Ry,x,Rz);
xlabel('Time(sec)');
ylabel('Rotation(degree)');
legend('Rx','Ry','Rz');
subplot(2,3,3);
plot(x,Fx,x,Fy,x,Fz);
xlabel('Time(sec)');
ylabel('Force(N)');
legend('Fx','Fy','Fz');
subplot(2,3,4);
plot(x,Mx,x,My,x,Mz);
xlabel('Time(sec)');
ylabel('Moment(Nm)');
legend('Mx','My','Mz');
subplot(2,3,[5,6]);
plot(Rx,My,'b');
xlabel('Rotation(degree)');
ylabel('Moment(Nm)');
hold on
plot(Rx(sp:ep),My(sp:ep),'r','line
width',2);

```

```
legend('Rx vs. Mx', 'Last  
cycle', 'location', 'southeast');
```

```
0.05 Hz, Intact FSU, Hybrid  
Position-load control');
```

```
sgtitle('\SN8DB003Rx5E2 -  
specimen 8, Flexion & Extension:
```

Appendix C Code of comparison plot

```
clear all;

% In this code, the stiffness,
% hysteresis zeroed loss
% area/coefficient and phase angle
% of impact

% discs before 25G needle injury
% was calculated.(SP8, SP10, SP12,
% SP14, SP16, SP18)

%LS = left stiffness, RS = right
% stiffness, HL = hysteresis zeroed
% loss area,

%HLc = Hysteresis zeroed loss
% area

% read the data

P8 =
textread('SN8DB003Rx5E2_P.txt');

L8 =
textread('SN8DB003Rx5E2_L.txt');

P10 =
textread('SN10DB003Rx5E2_P.txt
');

L10 =
textread('SN10DB003Rx5E2_L.txt'
);

P12 =
textread('SN12DB003Rx5E2_P.txt
');

L12 =
textread('SN12DB003Rx5E2_L.txt'
);

P14 =
textread('SN14DB003Rx5E2_P.txt
');

L14 =
textread('SN14DB003Rx5E2_L.txt'
);

P16 =
textread('SN16DB003Rx5E2_P.txt
');

L16 =
textread('SN16DB003Rx5E2_L.txt'
);

P18 =
textread('SN18DB003Rx5E2_P.txt
');

L18 =
textread('SN18DB003Rx5E2_L.txt'
);

P = [P8; P10; P12; P14; P16; P18];
```

```

L = [L8; L10; L12; L14; L16; L18];

Pn = P * (-1);

for n = 1:6:31
    Tx = P(n,:);
    Ty = P(n+1,:);
    Tz = P(n+2,:);
    Rx = P(n+3,:);
    Ry = P(n+4,:);
    Rz = P(n+5,:);

    Fx = L(n,:);
    Fy = L(n+1,:);
    Fz = L(n+2,:);
    Mx = L(n+3,:);
    My = L(n+4,:);
    Mz = L(n+5,:);
    Rxn = Rx * -1;

    %adjust the figure (by only
    moving Rz)

    Rx = Rx-(min(Rx)+max(Rx))/2;

    Rxn = Rxn-
    (min(Rxn)+max(Rxn))/2;

    % Find the last circle starting &
    ending location with Rz and Rzn

    [pks,locs] =
    findpeaks(Rx,'MinPeakDistance',5
    0,'MinPeakHeight',2);

    [pks1,locs1] =
    findpeaks(Rxn,'MinPeakDistance',
    50,'MinPeakHeight',2);

    sp = (locs(end-1)+locs1(end-
    1))/2; %find the last cycle starting
    point

    sp = round(sp);

    ep =
    (locs(end)+locs1(end))/2; %find
    the last cycle ending point

    ep = round(ep);

    RSr = find(Rx(sp:sp+0.25*(ep-
    sp))>1.5&Rx(sp:sp+0.25*(ep-
    sp))<2.9); %find the right stiffness
    1.5-2.9

    RSr = RSr+sp;

    RSr = round(RSr);

    LSr = find(Rx(sp+0.5*(ep-
    sp):sp+0.75*(ep-sp))>-
    2.9&Rx(sp+0.5*(ep-

```

```

sp):sp+0.75*(ep-sp))<-
1.5); %find the left stiffness

LSr = LSr+sp+0.5*(ep-sp);

LSr = round(LSr);

% Calculate the stiffness

PR = polyfit(Rx(RSr),Mx(RSr),1);

RS(n) = PR(1); %right stiffness

PL = polyfit(Rx(LSr),Mx(LSr),1);

LS(n) = PL(1); %left stiffness

% Find the zeroed Hysteresis
area

md = round((sp+ep)/2);

rq = round(sp+(ep-sp)/4);

lq = round(ep-(ep-sp)/4);

prt =
polyfit(Rx(sp:rq),Mx(sp:rq),9); %
right

xrt =
Rx(sp:rq); %top
equation

yrt = polyval(prt,xrt);

Art(n) = trapz(xrt,yrt);

prb =
polyfit(Rx(rq:md),Mx(rq:md),9);
%bottom equation

xrb = Rx(rq:md);

yrb = polyval(prb,xrb);

Arb(n) = trapz(xrb,yrb);

Ar(n) =
Art(n)+Arb(n); %
energy absorption at right

plb =
polyfit(Rx(md:lq),Mx(md:lq),9);
%left

xlb =
Rx(md:lq); %bottom
equation

ylb = polyval(plb,xlb);

Alb(n) = trapz(xlb,ylb);

plt =
polyfit(Rx(lq:ep),Mx(lq:ep),9); %t
op equation

xlt = Rx(lq:ep);

ylt = polyval(plt,xlt);

Alt(n) = trapz(xlt,ylt);

```

```

Al(n) = title('Before 25G')
Alb(n)+Alt(n); %
energy absorption at left

HL(n) =
Ar(n)+Al(n); %Hysteresis
zeroed area

HLc(n) =
HL/(Art+Alb); %Hysteresis
zeroed coefficient

% Phase angle
[phi, frq, cxy] = relphase(Rx,Mx);
PA(n) = phi;

% Plot the last cycle
X = [xrt,xrb,xlb,xlt];
Y = [yrt,yrb,ylb,ylt];
plot(X,Y,'LineWidth',2);
hold on;

legend('SN8','SN10','SN12','SN14',
'SN16','SN18','location','northwes
t');
xlabel('Rotation(degree)');
ylabel('Moment(Nm)');

RS = nonzeros(RS);
MeanRS = mean(RS);
SDRS = std(RS);

LS = nonzeros(LS);
MeanLS = mean(LS);
SDLS = std(LS);

HL = nonzeros(HL);
MeanHL = mean(HL);
SDHL = std(HL);

HLc = nonzeros(HLc);
MeanHLc = mean(HLc);
SDHLc = std(HLc);

PA = nonzeros(PA);
MeanPA = mean(PA);
SDPA = std(PA);

% Output the results into a excel
sheet
writematrix(RS,'Comparison_25G
_intact.xls','Sheet',1,'Range','A1');

```

```
writematrix(MeanRS,'Comparison_25G_intact.xls','Sheet',1,'Range','B1');
```

```
writematrix(SDRS,'Comparison_25G_intact.xls','Sheet',1,'Range','C1');
```

```
writematrix(LS,'Comparison_25G_intact.xls','Sheet',1,'Range','D1');
```

```
writematrix(MeanLS,'Comparison_25G_intact.xls','Sheet',1,'Range','E1');
```

```
writematrix(SDLS,'Comparison_25G_intact.xls','Sheet',1,'Range','F1');
```

```
writematrix(HL,'Comparison_25G_intact.xls','Sheet',1,'Range','G1');
```

```
writematrix(MeanHL,'Comparison_25G_intact.xls','Sheet',1,'Range','H1');
```

```
writematrix(SDHL,'Comparison_25G_intact.xls','Sheet',1,'Range','J1');
```

```
writematrix(HLc,'Comparison_25G_intact.xls','Sheet',1,'Range','K1');
```

```
writematrix(MeanHLc,'Comparison_25G_intact.xls','Sheet',1,'Range','L1');
```

```
writematrix(SDHLc,'Comparison_25G_intact.xls','Sheet',1,'Range','M1');
```

```
writematrix(PA,'Comparison_25G_intact.xls','Sheet',1,'Range','N1');
```

```
writematrix(MeanPA,'Comparison_25G_intact.xls','Sheet',1,'Range','O1');
```

```
writematrix(SDPA,'Comparison_25G_intact.xls','Sheet',1,'Range','P1');
```

Appendix D Code of overnight preload comparison

```

% Overload comparison between
before and after needle injury

% 25G group: S10 S12 S14 S16 S18

% 30G group: S7 S9 S11 S15 S17

clear all;

close all;

I_25G = textread('Before_25G.txt');
with a file order of 'L' 'P'

D_25G = textread('After_25G.txt');

I_30G = textread('Before_30G.txt');

D_30G = textread('After_30G.txt');

Incol{1} = 'b-'; %set linecolours for
linear regression of stiffness line
for a number of cycles

Incol{2} = 'g-';

Incol{3} = 'm-';

Incol{4} = 'c-';

Incol{5} = 'r-';

Incol{6} = 'b-'; %set linecolours for
linear regression of stiffness line
for a number of cycles

Incol{7} = 'g-';

Incol{8} = 'm-';

Incol{9} = 'c-';

Incol{10} = 'r-';

j = 1;

for n = 1:2:10

    Tz1 = nonzeros(I_25G(n,:))-
nonzeros(I_25G(n,1));

    Tzd1 = nonzeros(D_25G(n,:)) -
nonzeros(D_25G(n,1));

    figure(1)

    plot(Tz1,Incol{j},'linewidth',3);

    hold on;

    plot(Tzd1,Incol{j+5},'linewidth',1);

    hold on;

    legend('S10 intact','S10
damaged','S12 intact','S12

```

```

damaged','S14      intact','S14
damaged','S16      intact','S16
damaged','S18      intact','S18
damaged');

```

```

title('Fz Before and after 25G');

```

```

Tz2 = nonzeros(I_25G(n+1,:))-
nonzeros(I_25G(n+1,1));

```

```

Tzd2 = nonzeros(D_25G(n+1,:))
- nonzeros(D_25G(n+1,1));

```

```

figure(2)

```

```

plot(Tz2,Incol{j},'linewidth',3);

```

```

hold on;

```

```

plot(Tzd2,Incol{j+5},'linewidth',1);

```

```

hold on;

```

```

legend('S10      intact','S10
damaged','S12      intact','S12
damaged','S14      intact','S14
damaged','S16      intact','S16
damaged','S18      intact','S18
damaged');

```

```

title('Tz Before and after 25G');

```

```

Tz3 = nonzeros(I_30G(n,:))-
nonzeros(I_30G(n,1));

```

```

Tzd3 = nonzeros(D_30G(n,:)) -
nonzeros(D_30G(n,1));

```

```

figure(3)

```

```

plot(Tz3,Incol{j},'linewidth',3);

```

```

hold on;

```

```

plot(Tzd3,Incol{j+5},'linewidth',1);

```

```

hold on;

```

```

legend('S7      intact','S7
damaged','S9      intact','S9
damaged','S11      intact','S11
damaged','S15      intact','S15
damaged','S17      intact','S17
damaged');

```

```

title('Fz Before and after 30G');

```

```

Tz4 = nonzeros(I_30G(n+1,:))-
nonzeros(I_30G(n+1,1));

```

```

Tzd4 = nonzeros(D_30G(n+1,:))
- nonzeros(D_30G(n+1,1));

```

```

figure(4)

```

```

plot(Tz4,Incol{j},'linewidth',3);

```

```

hold on;

```

```

plot(Tzd4,Incol{j+5},'linewidth',1);

```

```

hold on;

```

```
legend('S7          intact','S7
damaged','S9          intact','S9
damaged','S11        intact','S11
damaged','S15        intact','S15
damaged','S17        intact','S17
damaged');

title('Tz Before and after 30G');

j = j+1;

end
```

Appendix E Phase angle calculation

```
function [phi, frq, cxy] =  
relphase(x,y,freq,show)
```

```
% RELPHASE finds the relative  
phase, PHI, between the vectors X  
and Y.
```

```
% The frequency, FRQ, and  
strength, CXY, of the coupling are  
also given.
```

```
% FREQ (optional, default is 2) is  
the sampling frequency of the  
vectors X and Y.
```

```
% SHOW (optional, default is do  
not show) plots the results if  
SHOW is input.
```

```
% Marcos Duarte  
mduarte@usp.br 22Jul2002
```

```
if ~exist('freq','var'), freq = 2; end
```

```
x = detrend(x);
```

```
y = detrend(y);
```

```
if length(x) > 1024 % you may have  
to find 'best' values for your case
```

```
    nfft = round(length(x)/2);
```

```
    nfft2 = 512;
```

```
elseif length(x) > 256
```

```
    nfft = 256;
```

```
    nfft2 = 256;
```

```
else
```

```
    nfft = length(x);
```

```
    nfft2 = length(x);
```

```
end
```

```
%nfft = 2^(nextpow2(length(x)));
```

```
%Cross Spectral Density of X and Y:
```

```
[Pxy,F] =  
csd(x,y,nfft,freq,nfft,round(nfft/2  
) , 'linear');
```

```
ang = angle(Pxy)*180/pi;
```

```
[m,i] = max(abs(Pxy));
```

```
%Phase between X and Y at their  
maximum cross-spectral density:
```

```
phi = ang(i);
```

```
frq = F(i);
```

```
%Coherence of X and Y  
(Coherence is a function of  
frequency with values
```

```
% between 0 and 1 that indicate  
how well X corresponds to Y at  
each frequency):
```

```

[Cxy,F2] = cohere(x,y,nfft2,freq,nfft2,round(
nfft2/2),'linear');

[tmp,i] = min(abs(F2-frq));

%Strength of the coupling:
cxy = Cxy(i);

%Plot:
if exist('show','var')
    figure
    subplot(3,1,1)
    plot(F,abs(Pxy),frq,m,'ro')
    ylabel('Cross Spectral Density')
    title(['Phase between X and Y: '
num2str(round(100*phi)/100),...
'^\circ' at '
num2str(round(100*frq)/100),...
' Hz with a coherence of '
num2str(round(100*cxy)/100)])
    subplot(3,1,2)
    plot(F2,Cxy,F2(i),cxy,'ro')
    xlabel('Frequency (Hz)')
    ylabel('Coherence')
    subplot(3,1,3)
    t
    =linspace(0,length(x)/freq,length(
x));
    plot(t,x,'k',t,y,'r')
    xlabel('Time (s)')
    ylabel('X and Y')
    legend('X','Y',0)
end

```

Appendix F t-test result of each DOF

Table F1. p value from t-test of each group

	Stiffness		Hysteresis loss area		Phase angle	
	25G group	30G group	25G group	30G group	25G group	30G group
Flexion						
Extension						
Right lateral bending	0.13	0.21	0.29	0.26	NA	0.37
Left Lateral Bending	0.45	0.44				
Right Axial Rotation	0.37	0.44	0.20	0.45	0.32	0.45
Left Axial Rotation	NA	0.26				
Right Lateral shear	0.31	0.34	0.49	0.28	NA	0.25
Left Lateral shear	0.22	0.37				
Anterior shear	0.048*	0.17	0.14	0.17	0.25	NA
Posterior shear	0.25	0.18				
Compression	0.26	0.27	NA	0.41	0.17	0.06

* indicates p value less than 0.05, where significant change occurs.

NA indicates t-test is not applicable due to its data is not normally distributed.

Based on Wilcoxon signed rank test,

- 25G group, lateral bending, phase angle, test statistic = 8 > critical value, no difference.
- 25G group, left axial rotation, stiffness, test statistic = 3 > critical value, no difference.
- 25G group, lateral shear, phase angle, test statistic = 5 > critical value, no difference.
- 30G group, anterior-anterior shear, phase angle, test statistic = 8 > critical value, no difference.
- 25G group, compression, hysteresis loss area, test statistic = 8 > critical value, no difference

Table F2. Measures of Skewness and Kurtosis before needle injury

Skewness Kurtosis	Stiffness		Hysteresis loss area		Phase angle	
	25G group	30G group	25G group	30G group	25G group	30G group
Flexion						
Extension						
Right lateral bending	0.97 1.88	0.49 -1.45	0.61 0.003	1.17 0.61	-0.84 0.57	0.96 0.78
Left Lateral Bending	0.65 0.19	-0.26 -1.18				
Right Axial Rotation	0.66 -1.05	-0.11 -0.75	-0.17 0.59	-0.31 -2.15	0.27 -1.32	0.30 -0.78
Left Axial Rotation	0.47 0.88	-0.65 -0.76				
Right Lateral shear	0.03 -0.58	0.40 -1.85	0.12 -1.88	0.50 0.12	1.86* 4.05*	-0.13 -2.22
Left Lateral shear	-0.53 -0.10	0.37 1.19				
Anterior shear	-0.26 -2.22	-0.56 0.27	0.26 -1.80	0.001 -0.15	-0.47 -2.34	0.31 0.84
Posterior shear	0.18 -2.08	0.25 0.51				
Compression	0.41 -1.48	-0.48 2.35	0.05 -0.03	-0.20 2.33	1.35 0.81	-0.63 -1.59

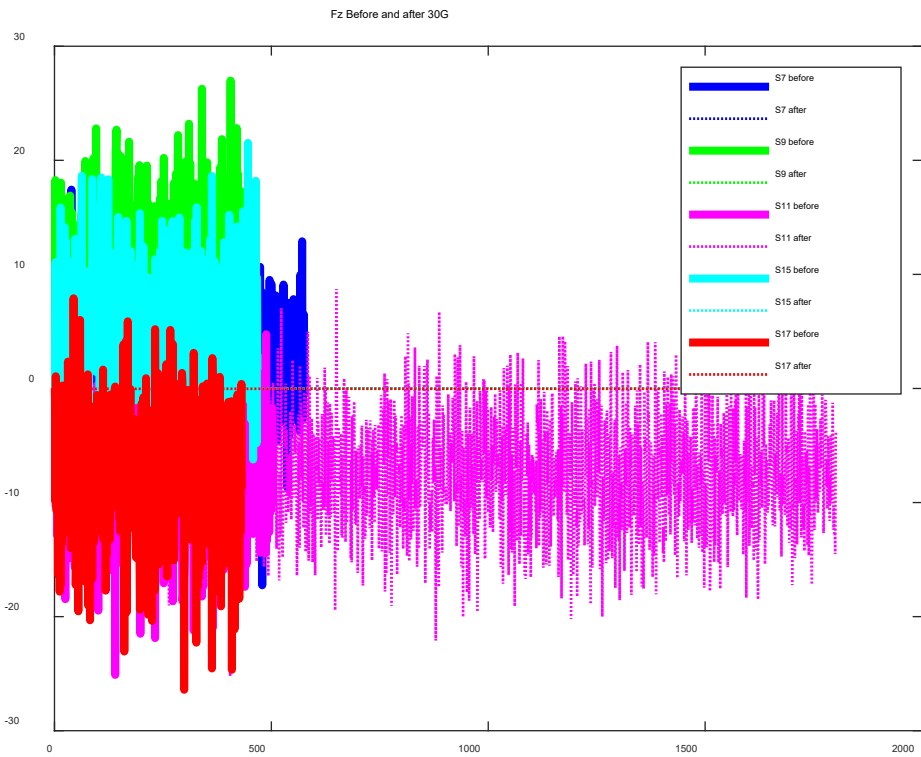
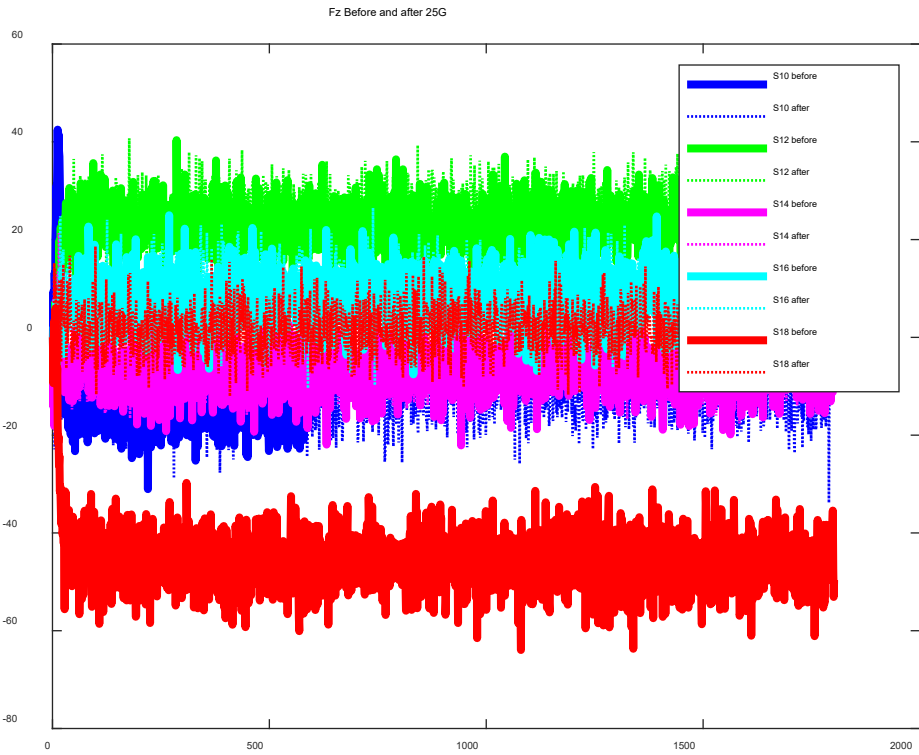
* indicates where data does not obey normal distribution.

Table F3. Measures of Skewness and Kurtosis after needle injury

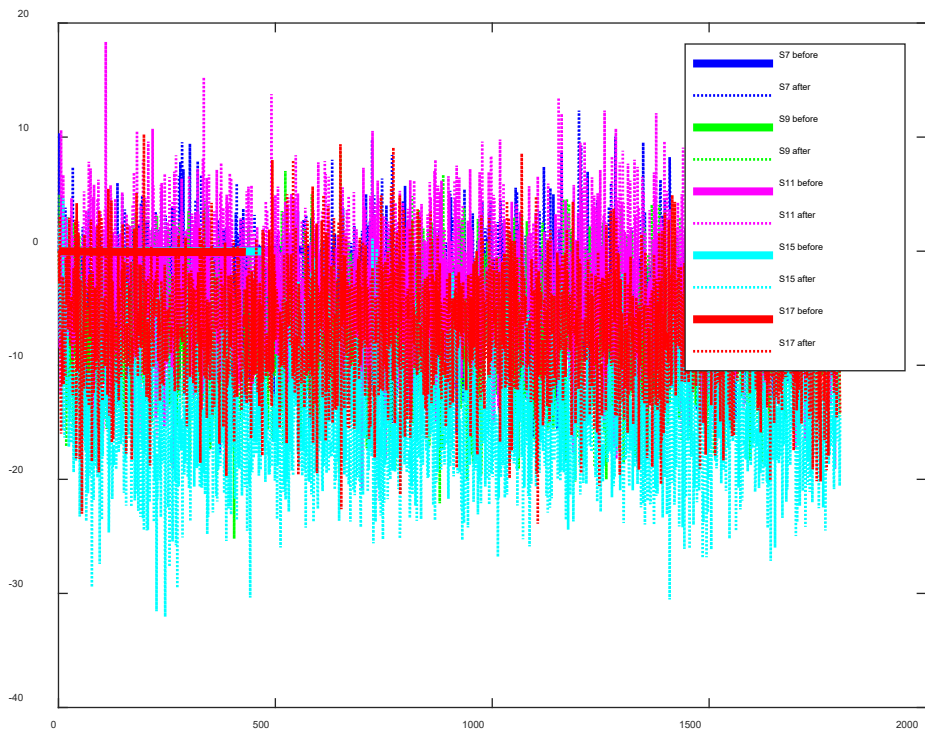
Skewness Kurtosis	Stiffness		Hysteresis loss area		Phase angle	
	25G group	30G group	25G group	30G group	25G group	30G group
Flexion						
Extension						
Right lateral bending	0.25 1.66	-0.40 -0.72	0.32	0.09	-1.41*	-0.72
Left Lateral Bending	0.57 0.99	-0.03 1.99	-1.06	-2.45	1.58	-1.69
Right Axial Rotation	0.07 -2.53	-0.94 0.17	-0.19	0.01	0.66	0.47
Left Axial Rotation	1.99* 4.01*	-0.46 2.01	-1.54	-0.47	-1.19	0.03
Right Lateral shear	0.14 -1.85	0.36 -0.86	0.93	-0.94	0.79	-0.39
Left Lateral shear	0.23 0.54	1.24 1.20	0.35	-1.86	0.44	0.77
Anterior shear	-0.67 -0.21	-0.98 0.61	-0.34	0.10	-0.76	1.62*
Posterior shear	0.62 -1.38	-0.81 -0.55	-2.01	-0.47	-1.70	2.88
Compression	-0.71 1.19	-0.97 -0.76	1.42* 1.77	0.64 -1.66	0.79 -0.78	-0.27 -0.16

* indicates where data does not obey normal distribution.

Appendix G Displacement over time and force over time plot of overnight compressive preload



Tz Before and after 30G



Reference

¹ Walker, J., El Abd, O., Isaac, Z., & Muzin, S. (2008). Discography in practice: a clinical and historical review. *Current reviews in musculoskeletal medicine*, 1(2), 69-83.

² Masuda, K., Aota, Y., Muehleman, C., Imai, Y., Okuma, M., Thonar, E. J., ... & An, H. S. (2005). A novel rabbit model of mild, reproducible disc degeneration by an annulus needle puncture: correlation between the degree of disc injury and radiological and histological appearances of disc degeneration. *Spine*, 30(1), 5-14.

³ Wang, J. L., Tsai, Y. C., & Wang, Y. H. (2007). The leakage pathway and effect of needle gauge on degree of disc injury post annular puncture: a comparative study using aged human and adolescent porcine discs. *Spine*, 32(17), 1809-1815.

⁴ Martin, J. T., Gorth, D. J., Beattie, E. E., Harfe, B. D., Smith, L. J., & Elliott, D. M. (2013). Needle puncture injury causes acute and long-term mechanical deficiency in a mouse model of intervertebral disc degeneration. *Journal of Orthopaedic Research*, 31(8), 1276-1282.

⁵ Huang, X., Wang, W., Meng, Q., Yu, L., Fan, C., Yu, J., ... & Ye, X. (2019). Effect of needle diameter, type and volume of contrast agent on intervertebral disc degeneration in rats with discography. *European Spine Journal*, 28(5), 1014-1022.

⁶ Alini, M., Eisenstein, S. M., Ito, K., Little, C., Kettler, A. A., Masuda, K., ... & Wilke, H. J. (2008). Are animal models useful for studying human disc disorders/degeneration?. *European Spine Journal*, 17(1), 2-19.

⁷ O'Connell, G. D., Vresilovic, E. J., & Elliott, D. M. (2007). Comparison of animals used in disc research to human lumbar disc geometry. *Spine*, 32(3), 328-333.

-
- ⁸ Beckstein, J. C., Sen, S., Schaer, T. P., Vresilovic, E. J., & Elliott, D. M. (2008). Comparison of animal discs used in disc research to human lumbar disc: axial compression mechanics and glycosaminoglycan content. *Spine*, *33*(6), E166-E173.
- ⁹ Showalter, B. L., Beckstein, J. C., Martin, J. T., Beattie, E. E., Orías, A. A. E., Schaer, T. P., ... & Elliott, D. M. (2012). Comparison of animal discs used in disc research to human lumbar disc: torsion mechanics and collagen content. *Spine*, *37*(15), E900.
- ¹⁰ Elliott, D. M., Yerramalli, C. S., Beckstein, J. C., Boxberger, J. I., Johannessen, W., & Vresilovic, E. J. (2008). The effect of relative needle diameter in puncture and sham injection animal models of degeneration. *Spine*, *33*(6), 588-596.
- ¹¹ Panjabi, M. M., & White, A. A. (1990). Clinical biomechanics of the spine.
- ¹² Carragee, E. J., Don, A. S., Hurwitz, E. L., Cuellar, J. M., Carrino, J., & Herzog, R. (2009). 2009 ISSLS prize winner: does discography cause accelerated progression of degeneration changes in the lumbar disc: a ten-year matched cohort study. *Spine*, *34*(21), 2338-2345.
- ¹³ Hartman, R. A., Bell, K. M., Quan, B., Nuzhao, Y., Sowa, G. A., & Kang, J. D. (2015). Needle puncture in rabbit functional spinal units alters rotational biomechanics. *Journal of spinal disorders & techniques*, *28*(3), E146.
- ¹⁴ Korecki, C. L., Costi, J. J., & Iatridis, J. C. (2008). Needle puncture injury affects intervertebral disc mechanics and biology in an organ culture model. *Spine*, *33*(3), 235.
- ¹⁵ Keorochana, G., Johnson, J. S., Taghavi, C. E., Liao, J. C., Lee, K. B., Yoo, J. H., ... & Wang, J. C. (2010). The effect of needle size inducing degeneration in the rat caudal disc: evaluation using radiograph, magnetic resonance imaging, histology, and immunohistochemistry. *The spine journal*, *10*(11), 1014-1023.
- ¹⁶ Australian institute of health and welfare (AIHW), review on 3 May 2020, <
<https://www.aihw.gov.au/reports/chronic-musculoskeletal-conditions/back-problems/contents/what-are-back-problems> >

-
- ¹⁷ Botwin, K. P., Fuoco, G. S., Torres, F. M., Gruber, R. D., Bouchlas, C. C., Castellanos, R., & Rao, S. (2003). Radiation exposure to the spinal interventionalist performing lumbar discography. *Pain Physician, 6*(3), 295-300.
- ¹⁸ Iatridis, J. C., & Hecht, A. C. (2012). Commentary: Does needle injection cause disc degeneration? News in the continuing debate regarding pathophysiology associated with intradiscal injections. *The Spine Journal, 12*(4), 336-338.
- ¹⁹ Centerville, O. H., Niagara, W. I., Center, I. P., Woodbine, D., Manchikanti, L., Medtronic, S. I., & Stryker, N. (2018). An update of the systematic appraisal of the accuracy and utility of discography in chronic spinal pain. *Pain physician, 21*(2), 91-110.
- ²⁰ Walsh, T. R., Weinstein, J. N., Spratt, K. F., Lehmann, T. R., Aprill, C., & Sayre, H. (1990). Lumbar discography in normal subjects. A controlled, prospective study. *The Journal of bone and joint surgery. American volume, 72*(7), 1081-1088.
- ²¹ Manchikanti, L., Kaye, A. D., Falco, F. J., & Hirsch, J. A. (Eds.). (2018). *Essentials of Interventional Techniques in Managing Chronic Pain*. Springer.
- ²² Cohen, S. P., Larkin, T. M., Barna, S. A., Palmer, W. E., Hecht, A. C., & Stojanovic, M. P. (2005). Lumbar discography: a comprehensive review of outcome studies, diagnostic accuracy, and principles.
- ²³ Michalek, A. J., Buckley, M. R., Bonassar, L. J., Cohen, I., & Iatridis, J. C. (2010). The effects of needle puncture injury on microscale shear strain in the intervertebral disc annulus fibrosus. *The Spine Journal, 10*(12), 1098-1105.
- ²⁴ Carragee, E. J., Don, A. S., Hurwitz, E. L., Cuellar, J. M., Carrino, J., & Herzog, R. (2009). 2009 ISSLS prize winner: does discography cause accelerated progression of degeneration changes in the lumbar disc: a ten-year matched cohort study. *Spine, 34*(21), 2338-2345.
- ²⁵ van Heeswijk VM, Thambyah A, Robertson PA, Broom ND. Does an Annular Puncture Influence the Herniation Path?: An In Vitro Mechanical and Structural

Investigation. *Spine* (Phila Pa 1976). 2018;43(7):467–476.
doi:10.1097/BRS.0000000000002336

²⁶ Crevensten, G., Walsh, A. J., Ananthakrishnan, D., Page, P., Wahba, G. M., Lotz, J. C., & Berven, S. (2004). Intervertebral disc cell therapy for regeneration: mesenchymal stem cell implantation in rat intervertebral discs. *Annals of biomedical engineering*, 32(3), 430-434.

²⁷ Anderson, D. G., Li, X., Tannoury, T., Beck, G., & Balian, G. (2003). A fibronectin fragment stimulates intervertebral disc degeneration in vivo. *Spine*, 28(20), 2338-2345.

²⁸ Okuma, M., Mochida, J., Nishimura, K., Sakabe, K., & Seiki, K. (2000). Reinsertion of stimulated nucleus pulposus cells retards intervertebral disc degeneration: an in vitro and in vivo experimental study. *Journal of Orthopaedic Research*, 18(6), 988-997.

²⁹ Han, B., Zhu, K., Li, F. C., Xiao, Y. X., Feng, J., Shi, Z. L., ... & Chen, Q. X. (2008). A simple disc degeneration model induced by percutaneous needle puncture in the rat tail. *Spine*, 33(18), 1925-1934.

³⁰ Liang, H., Ma, S. Y., Feng, G., Shen, F. H., & Li, X. J. (2010). Therapeutic effects of adenovirus-mediated growth and differentiation factor-5 in a mice disc degeneration model induced by annulus needle puncture. *The Spine Journal*, 10(1), 32-41.

³¹ Hartman, R. A., Bell, K. M., Quan, B., Nuzhao, Y., Sowa, G. A., & Kang, J. D. (2015). Needle puncture in rabbit functional spinal units alters rotational biomechanics. *Journal of spinal disorders & techniques*, 28(3), E146.

³² Jay Lipson, S., & Muir, H. (1981). Experimental intervertebral disc degeneration. Morphologic and proteoglycan changes over time. *Arthritis & Rheumatism: Official Journal of the American College of Rheumatology*, 24(1), 12-21.

³³ O'Connell, G. D., Vresilovic, E. J., & Elliott, D. M. (2007). Comparison of animals used in disc research to human lumbar disc geometry. *Spine*, 32(3), 328-333.

-
- ³⁴ Wilke, H. J., Kettler, A., & Claes, L. E. (1997). Are sheep spines a valid biomechanical model for human spines?. *Spine*, 22(20), 2365-2374.
- ³⁵ Reid, J. E., Meakin, J. R., Robins, S. P., Skakle, J. M. S., & Hukins, D. W. L. (2002). Sheep lumbar intervertebral discs as models for human discs. *Clinical Biomechanics*, 17(4), 312-314.
- ³⁶ Chamoli, U., Umali, J., Kleuskens, M. W., Chepurin, D., & Diwan, A. D. (2019). Morphological characteristics of the kangaroo lumbar intervertebral discs and comparison with other animal models used in spine research. *European Spine Journal*, 1-11.
- ³⁷ Wade, K. R., Robertson, P. A., Thambyah, A., & Broom, N. D. (2015). "Surprise" loading in flexion increases the risk of disc herniation due to annulus-endplate junction failure: a mechanical and microstructural investigation. *Spine*, 40(12), 891-901.
- ³⁸ MAYO foundation for medical education and research.
- ³⁹ Walker, J., El Abd, O., Isaac, Z., & Muzin, S. (2008). Discography in practice: a clinical and historical review. *Current reviews in musculoskeletal medicine*, 1(2), 69-83.
- ⁴⁰ Botwin, K. P., Fuoco, G. S., Torres, F. M., Gruber, R. D., Bouchlas, C. C., Castellanos, R., & Rao, S. (2003). Radiation exposure to the spinal interventionalist performing lumbar discography. *Pain Physician*, 6(3), 295-300.
- ⁴¹ McCulloch, J. A., & Waddell, G. (1978). Lateral lumbar discography. *The British journal of radiology*, 51(607), 498-502.
- ⁴² Russo, M. P., Ciric, D., Amin, D. B., & Costi, J. J. *LUMBAR DISC HERNIATION FAILURE AFTER MULTIAXIAL FATIGUE.*
- ⁴³ Amin, D. B., Sommerfeld, D., Lawless, I. M., Stanley, R. M., Ding, B., & Costi, J. J. (2016). Effect of degeneration on the six degree of freedom mechanical properties

of human lumbar spine segments. *Journal of Orthopaedic Research*, 34(8), 1399-1409.

⁴⁴ Pflaster, D. S., Krag, M. H., Johnson, C. C., Haugh, L. D., & Pope, M. H. (1997). Effect of test environment on intervertebral disc hydration. *Spine*, 22(2), 133-139.

⁴⁵ Race, A., Broom, N. D., & Robertson, P. (2000). Effect of loading rate and hydration on the mechanical properties of the disc. *Spine*, 25(6), 662-669.

⁴⁶ Costi, J. J., Stokes, I. A., Gardner-Morse, M. G., & Iatridis, J. C. (2008). Frequency-dependent behavior of the intervertebral disc in response to each of six degree of freedom dynamic loading: solid phase and fluid phase contributions. *Spine*, 33(16), 1731.

⁴⁷ Edwards, W. T., Ordway, N. R., Zheng, Y., McCullen, G., Han, Z., & Yuan, H. A. (2001). Peak stresses observed in the posterior lateral anulus. *Spine*, 26(16), 1753-1759.

⁴⁸ Nachemson, A. L. F., & Morris, J. M. (1964). In vivo measurements of intradiscal pressure: discometry, a method for the determination of pressure in the lower lumbar discs. *JBJS*, 46(5), 1077-1092.

⁴⁹ Lawless, I. M., Ding, B., Cazzolato, B. S., & Costi, J. J. (2014). Adaptive velocity-based six degree of freedom load control for real-time unconstrained biomechanical testing. *Journal of biomechanics*, 47(12), 3241-3247.

⁵⁰ Michalek, A. J., Funabashi, K. L., & Iatridis, J. C. (2010). Needle puncture injury of the rat intervertebral disc affects torsional and compressive biomechanics differently. *European Spine Journal*, 19(12), 2110-2116.

⁵¹ Anderson, D. G., Li, X., Tannoury, T., Beck, G., & Balian, G. (2003). A fibronectin fragment stimulates intervertebral disc degeneration in vivo. *Spine*, 28(20), 2338-2345.

⁵² Boxberger, J. I., Sen, S., Yerramalli, C. S., & Elliott, D. M. (2006). Nucleus pulposus glycosaminoglycan content is correlated with axial mechanics in rat lumbar motion segments. *Journal of orthopaedic research*, 24(9), 1906-1915.